INVESTIGATION OF MAXIMUM WIRELESS POWER TRANSFER CONDITIONS IN THE NEAR FIELD
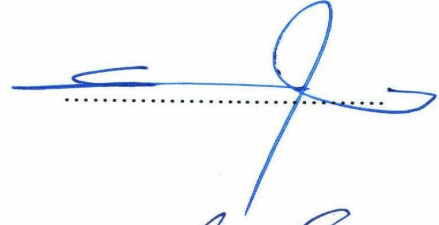
by
Nuri TEMÜRLENK

Submitted to the Institute of Graduate Studies in
Science and Engineering in partial fulfillment of
the requirements for the degree of
Masters of Science
in
Electrical and Electronics Engineering

Yeditepe University
2010

INVESTIGATION OF MAXIMUM WIRELESS POWER TRANSFER
CONDITIONS IN THE NEAR FIELD

APPROVED BY:

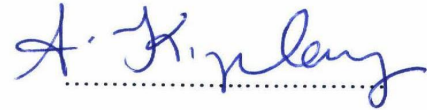Inst. Dr. Cahit CANBAY

(Thesis Supervisor)

Prof. Dr Hüseyin Selçuk VAROL

Assoc. Prof. Dr. Ahmet KIZILAY

DATE OF APPROVAL: 20 / 01 / 2010

ACKNOWLEDGEMENTS

ABSTRACT

INVESTIGATION OF MAXIMUM WIRELESS POWER TRANSFER CONDITIONS IN THE NEAR FIELD

This study discusses the theory and design of coupled resonant power transmission scheme and how array coupled wireless transmission of electrical power. Detailed simulation and analysis of near and radiation field, gain, Q factor, efficiency of transmission and radiator form comparisons will be studied while changing various radiator and medium parameters. Detailed derivation of operational theory and frequency and time domain calculations of coupled resonating RLC circuits will be presented. Application of negative resistance oscillator and ultra-wideband oscillators and various techniques for determining resonant frequency under dynamic loading conditions will be discussed. Configuration of radiator arrays for maximum power transfer conditions, analysis of mutual coupling between the array elements will be studied for optimum performance analysis of the antenna. All antenna parameters will be determined and compared with the experimental measurements of the antenna.

ÖZET

EN İYİ YAKIN ALAN KABLOSUZ GÜÇ TRANSFERİ KOŞULLARININ ARAŞTIRILMASI

Bu çalışma rezonant eşlenik kablosuz güç iletimi ve dizi eşlenik kablosuz güç iletimi sisteminin tasarımı ve teorisi üzerine yapılmıştır. Ortam ve radyatör yapısal parametrelerini değiştirerek yakın ve uzak alan, kazanç, Q katsayısı, güç iletim verimliliği ve radyatör form tasarımı detaylı analiz ve simülasyonlar yapılarak çalışılacaktır. Eşlenik rezonant RLC devre modeli kullanılarak sistemin çalışma teorisi, detaylı frekans ve zaman uzayı hesapları yapılarak türetilecektir. Negatif dirençli, çok-geniş-bantlı osilatörler ve değişken yüklenme koşullarında rezonant frekansın değişmesi tartışılacaktır. Çoklu radyatör dizilerinin en üst güç transferi için ayarlanması, dizi elemanları arasında bağıl eşlenmenin analizi en optimum anten performansını sağlamak için yapılacaktır. Tüm anten parametreleri hesaplanarak deneysel sonuçlar ile karşılaştırılacaktır.

TABLE OF CONTENTS

LIST OF FIGURES

LIST OF TABLES

SYMBOLS AND ABBREVIATIONS

$\vec{A}$	Magnetic Vector Potential
$\vec{B}$	Magnetic Flux Density
C	Capacitance
E	Energy
$\vec{H}$	Magnetic Field Intensity
f	Frequency
fo	Natural Resonance or Self Resonance Frequency
$\vec{J}(r,t)$	Current Density (A/m2)
k	Coupling Coefficient
L	Inductance
M	Mutual Inductance
P	Power
R	Resistance
Q	Quality Factor
X_C	Capacitive Reactance
X_L	Inductive Reactance
α	Attenuation Constant
β	Phase Constant
ξ	Damping Coefficient
ε	Permittivity $\varepsilon = \varepsilon_0 \varepsilon_r$
ε_0	Permittivity of space $8.854 \times 10^{-12} F/m$
ε_r	Relative Permittivity $\varepsilon_r = \varepsilon_r{}' - j\varepsilon_r{}''$
η	Efficiency
ρ	Charge Density
σ	Conductivity
δ	Skin Depth

τ	Discharge time
μ	Permeability $\mu = \mu_0 \mu_r$
μ_0	Permeability of space $4\pi \times 10^{-7} H/m$
μ_r	Relative Permeability $\mu_r = \mu_r' - j\mu_r''$
ω	Angular frequency $2\pi f$
γ	Propagation constant
Φ	Magnetic Flux
$\vec{\nabla}$	Delta Operator (Gradient)
$\vec{\nabla}\cdot$	Divergence Operator
$\vec{\nabla}\times$	Curl Operator
AC	Alternating Current
BW	Bandwidth
DC	Direct Current
EM	Electro Magnetic
MHz	Mega Hertz
$OSHA$	Occupational Safety and Health Administration
RF	Radio Frequency
$VSWR$	Voltage Standing Wave Ratio
UAV	Unmanned Aero Vehicle
QWR	Quarter Wave Resonator

1. INTRODUCTION

1.1. STATEMENT OF PROBLEM

Power is important to modern systems. From the smallest sensors, bionic implants, laptops, consumer products to satellites and oil platforms, it is important to be able to deliver power means other than classical wires or transmission lines. Wireless transmission is useful in cases where instantaneous or continuous energy transfer is needed but interconnecting wires are inconvenient, hazardous, or impossible. In the case of biological implants, there must be a battery or energy storage element present that can receive and hold energy. This element takes up valuable space inside a person body. In the case of satellites, UAVs and oil platforms, solar panels, fuel cells, or combustion engines are currently used to supply power. Solar panels take up a great deal of weight and bulk in terms of energy density and must have a tracking system to maximize exposure to the sun. Fuel cells and combustion cells needs fuel and maintenance to be delivered on site.

This thesis studies the theory, design, and construction of a method to transmit wireless electrical power through space. Investigation of various geometrical and physical form factors evaluated in order to increase coupling between transmitter and receiver. An array structure is also presented in order to utilize wider spectrum while utilizing same physical radiator and receiver space. Use of resonant coupling in order to maximize power transfer and analytical derivations of coupled network power transfer calculations is presented.

This thesis is broken down into three subsequent chapters. The first chapter starts with the introduction of wireless power transmission in nature, historical developments and motivations to develop near field high power wireless power transmission systems. The second chapter discusses about the selection of radiators and receiver for near field inductive transmission and loop radiator design for DC and AC conditions. The third chapter discusses about coupled network theorem and calculation of mutual inductance relations. The fourth

chapter discusses about array structures and methods of maximizing power transmission by means of utilizing wide spectrum.

1.2. HISTORY OF WIRELESS POWER TRANSMISSION

Magnetic fields and inductive coupling have been studied since the discovery of transformer by Hans Oersted and Michael Faraday. In 1886, Westinghouse Company developed first commercial AC transformer.

A complete mathematical understanding of the coupled circuits used to make the transmitter and receiver was first published by Frederick Terman in 1935.

Idea of using microwave power transmission was put forward by William C. Brown in 1961.

In 1973, world first passive RFID system demonstrated at Los-Alamos National Lab.

In 1988, a power electronics group led by Prof. John Boys at The University of Auckland in New Zealand, developed an inverter using novel engineering materials and power electronics and concludes that inductive power transmission should be achievable. A first prototype for a contact-less power supply is built.

In 2007, a physics research group, led by Prof. Marin Soljačić, at MIT confirm the earlier (1980's) work of Prof. Boys by wireless powering of a 60W light bulb with 40% efficiency at a 2 meters distance using two 60 cm-diameter coils.

In 2010, Haier Group debuts the world's first completely wireless LCD television at CES 2010 based on Prof. Marin Soljacic's research on wireless energy transfer and Wireless Home Digital Interface (WHDI).

1.3. MOTIVATION

Wireless energy transfer by radiation of electromagnetic waves and particles is also how nature transmits power to remote locations. There is a great harmony of power distribution from huge radiators (e.g. stars, sun) to receptors (earth, plants, heat transfer) in nature. If we take nuclear explosions and other reactions in stars as power source, we find almost whole spectrum is being utilized as power transmission medium. From very low frequencies up to particles can be assumed as source of energy. Harmony of emissions and receptions create us a great environment to survive. If we take earth system as a receiver, we find each part of layers in atmosphere receives some portion of spectra; lakes, seas, plants, down to core of earth; waves and particles carry power and bring to the receivers. This model of wireless power transmission in nature helped humanity to understand how artificial wave sources can be designed and utilized for transmission of power and information.

Race of wireless power transmission started with Dr. Nikola Tesla in 1880s. There is tremendous interest in wireless devices and gadgets in 21. Century, with the compactness of such devices created a need for cord-less charging systems. Even busses, trains, cars are becoming electric driven. Electric drive offers lower cost fuel, compactness and better regenerative use of fuel. Besides all these advantages, high density electric storage is still very challenging task. Because either recharging rate and life or energy density of existing battery and super capacitor systems are not sufficient to meet industrial criteria's.

Near field wireless transmission is a technique over distances comparable to, or a few times the diameter of the devices, and up to around a quarter of the wavelengths used [1]. Near field energy itself is non radiative, but some radiative losses will occur. In addition there are usually resistive losses. Near field transfer is usually magnetic (inductive), but electric (capacitive) energy transfer can also occur [2]. We restrict our studies in the near field power transmission systems.

2. SELECTION OF RADIATOR AND RECEIVER ELEMENTS

Wireless energy transfer or wireless power transmission is the process that takes place in any system where electrical energy is transmitted from a power source to an electrical load without interconnecting wires. The most common form of wireless power transmission is carried out using induction, followed by electro-dynamic induction. Other technologies for wireless power include those based on microwaves and lasers. Compared to inductive transfer in transformers, except when the coils are well within a diameter of each other, the efficiency is somewhat lower (around 80% at short range) whereas conventional transformers may achieve greater efficiency (around 90-95%), and for this reason, it's unlikely it will be used very much at larger distances where high energy is transferred [3].

However, compared to the costs associated with batteries, particularly non rechargeable batteries, the costs of the batteries are hundreds of times higher. In situations where a source of power is available nearby, it can be a cheaper solution. In addition, whereas batteries need periodic maintenance and replacement, resonant energy transfer could be used instead, which would not need this. Batteries additionally generate pollution during their construction and their disposal which largely would be avoided.

2.1. INDUCTIVE POWER TRANSMISSION

The action of an electrical transformer is the simplest instance of wireless energy transfer. The primary and secondary circuits of a transformer are not directly connected. The transfer of energy takes place by electromagnetic coupling through a process known as mutual induction. An added benefit is the capability to step the primary voltage either up or down. The battery charger of a mobile phone or the transformers in the street is examples of how this principle can be used. Induction cookers and many electric toothbrushes are also powered by this technique.

The main drawback to induction, however, is the short range. The receiver must be very close to the transmitter or induction unit in order to inductively couple with it.

The "electro-dynamic inductive effect" or "resonant inductive coupling" has key implications in solving the main problem associated with non-resonant inductive coupling and electromagnetic radiation for wireless energy transfer; specifically, the dependence of efficiency on transmission distance. [4-7] Electromagnetic induction works on the principle of a transmitter coil generating a predominantly magnetic field and a receiver coil being within that field so a current is induced in the receiver. This results in a relatively short range because most of the magnetic field misses the receiver. Over greater distances the non-resonant induction method is inefficient and wastes much of the transmitted energy.

Inductive power radiator is different than classical far field radiation. It is aimed to have more inductive power transmission than radiative. We generalize total transmission success of resonant system by a generic formula;

$$G_{Success} = e\left(D_{directivity} + D_{dis\tan ce} + D_{compatability}\right) \qquad (2.1)$$

Where $G_{Success}(1,...,\infty)$ is a success measure of all conditions and parameters which effect complete system performance, $e(0,...,1)$ is efficiency, $D_{directivity}(1,...,\infty)$ is directional success factor which is a function of transmitter and receiver crossing flux surface and angle, $D_{dis\tan ce}(0,...,x)$ is a distance success factor and it is inversely proportional with transmitter and receiver distance, $D_{compatability}(0,...,1)$ is a very integrated compatibility success factor which is function of electrical (dc, ac resistance, self inductance, self capacitance, resonant frequency, bandwidth etc..), geometrical (wire diameter, inter-winding distance, height, number of turns and length of wire), physical compatibility (conductive material and medium parameters, temperature, pressure) of couples. $D_{compatability}$ is also a function of applied frequency and transmitting and receiving systems' resonant frequencies.

We define efficiency as;

$$e = \frac{P_{rec}^{tot} - P_{loss}^{tot}}{P_{trans}^{tot}}$$

(2.2)

Where P_{trans}^{tot} is the total transmitted inductive and radiative power. Efficiency takes values between $e(-\infty...0,...+\infty)$, thus we can say if the power received is less than %50 of the transmitted power, than system is unsuccessful. In order to be successful, received power must be greater than half of the transmitted power.

In the next chapter we start from basic magneto-static electromagnetic field calculations in order to integrate most of the parameters which impact success parameters.

2.2. MAGNETOSTATIC FIELD ANALYSIS OF LOOP RADIATOR
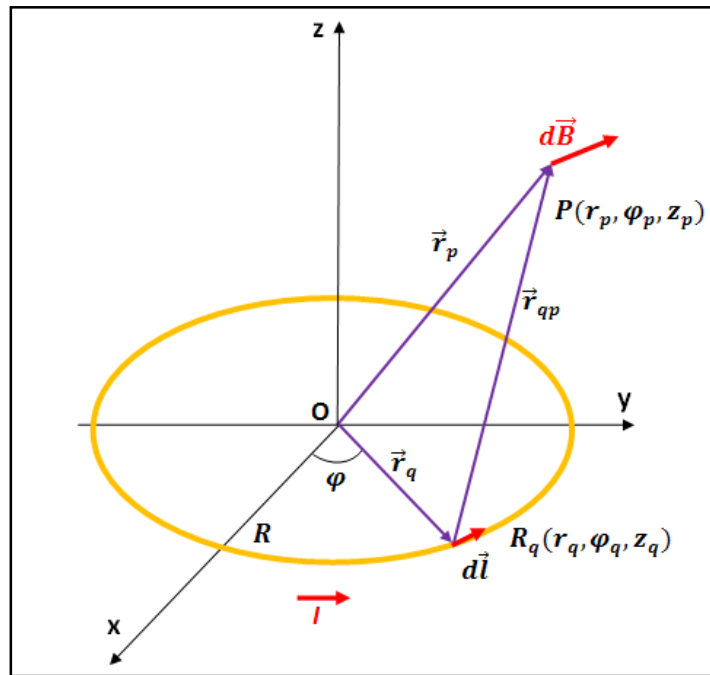
Figure 2.1. Circular thin wire loop located co-axially with z-axis

We first derive equations from the DC conditions and apply vector potential approach to derive near field wave equations to integrate dispersive characteristics of medium [8, 9, 10].

Magnetic field density of thin wire circular loop of radius R lying in the x-y plane and carrying a steady current I, at arbitrary point P is calculated using Biot-Savart Law in Cartesian coordinates and vector potential approach in cylindrical coordinates [11].

$$\vec{r_q} = R(\cos\varphi_q \vec{a}_x + \sin\varphi_q \vec{a}_y + 0\vec{a}_z) \qquad (2.3)$$

The differential current element is

$$d\vec{l} = (\frac{d\vec{r_q}}{d\varphi_q})d\varphi_q = R(-\sin\varphi_q \vec{a}_x + \cos\varphi_q \vec{a}_y)d\varphi_q \qquad (2.4)$$

$$\vec{r_p} = r_p(\cos\varphi_p \vec{a}_x + \sin\varphi_p \vec{a}_y + \vec{a}_z) \qquad (2.5)$$

Relative position vector is

$$\vec{r}_{qp} = \left[(r_p\cos\varphi_p - R\cos\varphi_q)\vec{a}_x + (r_p\sin\varphi_p - R\sin\varphi_q)\vec{a}_y + r_p\vec{a}_z\right] \qquad (2.6)$$

And the unit vector

$$\vec{a}_{qp} = \frac{\vec{r}_{qp}}{r_{qp}} = \frac{\vec{r_p} - \vec{r_q}}{|\vec{r_p} - \vec{r_q}|} \qquad (2.7)$$

$d\vec{l} \times \vec{r}_{qp}$ cross product

$$d\vec{l} \times \vec{r}_{qp} = \left[R(-\sin\varphi_q \vec{a}_x + \cos\varphi_q \vec{a}_y)d\varphi_q \right] \times$$
$$\left[(r_p \cos\varphi_p - R\cos\varphi_q)\vec{a}_x + (r_p \sin\varphi_p - R\sin\varphi_q)\vec{a}_y + r_p \vec{a}_z \right] \tag{2.8}$$

The contribution of the current element to the magnetic field at P is

$$d\vec{B} = \frac{\mu_0 I}{4\pi} \frac{d\vec{l} \times \vec{a}_{qp}}{\left| r_{qp} \right|^2} = \frac{\mu_0 I}{4\pi} \frac{d\vec{l} \times \vec{r}_{qp}}{\left| r_{qp} \right|^3} \tag{2.9}$$

Plugging terms

$$d\vec{B} = \frac{\mu_0 IR}{4\pi} \frac{\left[\begin{array}{c} (r_p \sin\varphi_p - R\sin\varphi_q)(r_p)\vec{a}_x \\ +(\sin\varphi_q r_p)\vec{a}_y \\ +\left(\begin{array}{c} (-\sin\varphi_q)(r_p \sin\varphi_p - R\sin\varphi_q) \\ -(\cos\varphi_q)(r_p \cos\varphi_p - R\cos\varphi_q) \end{array} \right)\vec{a}_z \end{array} \right]}{\left[\begin{array}{c} (r_p \cos\varphi_p - R\cos\varphi_q)^2 \\ +(r_p \sin\varphi_p - R\sin\varphi_q)^2 + r_p^2 \end{array} \right]^{\frac{3}{2}}} d\varphi_q \tag{2.10}$$

The x, y and the z components of Magnetic flux density at P is

$$\vec{B}_x = \vec{a}_x \frac{\mu_0 IR r_p}{4\pi} \int_0^{2\pi} \frac{r_p \sin\varphi_p - R\sin\varphi_q}{\left[(r_p \cos\varphi_p - R\cos\varphi_q)^2 + (r_p \sin\varphi_p - R\sin\varphi_q)^2 + r_p^2 \right]^{\frac{3}{2}}} d\varphi_q \tag{2.11}$$

$$\vec{B}_y = \vec{a}_y \frac{\mu_0 IR r_p}{4\pi} \int_0^{2\pi} \frac{\sin\varphi_q}{\left[(r_p \cos\varphi_p - R\cos\varphi_q)^2 + (r_p \sin\varphi_p - R\sin\varphi_q)^2 + r_p^2 \right]^{\frac{3}{2}}} d\varphi_q \tag{2.12}$$

$$\vec{B}_z = \vec{a}_z \frac{\mu_0 I R}{4\pi} \int_0^{2\pi} \frac{\begin{pmatrix} (-\sin\varphi_q)(r_p \sin\varphi_p - R\sin\varphi_q) \\ -(\cos\varphi_q)(r_p \cos\varphi_p - R\cos\varphi_q) \end{pmatrix}}{\left[\begin{matrix} (r_p \cos\varphi_p - R\cos\varphi_q)^2 \\ +(r_p \sin\varphi_p - R\sin\varphi_q)^2 \\ +r_p^2 \end{matrix} \right]^{\frac{3}{2}}} d\varphi_q \tag{2.13}$$

2.2.1. Vector Potential Approach In Cylindrical Coordinates

The vector potential at any arbitrary point $P(r_p, \varphi_p, z_p)$ shown in Figure 2.1 is derived. From symmetry, we know that in cylindrical polar coordinates the magnitude of $\vec{A}$ is independent of φ. Therefore, for simplicity, we choose the point $P(r_p, \varphi_p, z_p)$ in the r-z plane where $\varphi = 0$.

We notice that when equidistant elements of length dl at $+\varphi$ and $-\varphi$ are paired, the resultant is normal to r-z plane. Thus, $\vec{A}$ has only the single component A_φ. Let dl_φ, be the component of dl in this direction,

$$A_\varphi = \frac{\mu_0 I}{4\pi} \oint \frac{dl_\varphi}{r_{qp}} \tag{2.14}$$

$$A_\varphi = \frac{\mu_0 I}{2\pi} \int_0^\pi \frac{R\cos\varphi \, d\varphi}{\sqrt{R^2 + r_p^2 + z_p^2 - 2Rr_p \cos\varphi}} \tag{2.15}$$

Let $\varphi = \pi + 2\theta$ so that $d\varphi = 2d\theta$ and $\cos\varphi = 2\sin^2\theta - 1$, then this becomes

$$A_\varphi = \frac{\mu_0 I R}{2\pi} \int_0^{\frac{\pi}{2}} \frac{\left(2\sin^2\theta - 1\right)d\theta}{\sqrt{\left(R + r_p\right)^2 + z_p^2 - 4Rr_p \sin^2\theta}} \tag{2.16}$$

Let

$$k^2 = \frac{4Rr_p}{(R+r_p)^2 + z^2} \tag{2.17}$$

And rearrange, we get

$$A_\varphi = \frac{k\mu_0 I}{2\pi}\left(\frac{R}{r_p}\right)^{\frac{1}{2}}\left[\left(\frac{2}{k^2}-1\right)\int_0^{\frac{\pi}{2}}\frac{d\theta}{\sqrt{1-k^2\sin^2\theta}} - \frac{2}{k^2}\int_0^{\frac{\pi}{2}}\sqrt{1-k^2\sin^2\theta}\,d\theta\right]$$

$$\tag{2.18}$$

$$= \frac{\mu_0 I}{\pi k}\left(\frac{R}{r_p}\right)^{\frac{1}{2}}\left[\left(1-\frac{k^2}{2}\right)K - E\right] = \frac{\mu_0 I}{32}\left(\frac{R}{r_p}\right)^{\frac{1}{2}}k^3\left(1+\frac{3}{4}k^2 + \frac{75}{128}k^4 + \cdots\right)$$

Where, K and E are complete elliptic integrals of the first and second kind. To determine the magnetic induction, we must write, from (A.04), (A.05), (A.06), and the components of the curl in cylindrical coordinates.

$$div\vec{A} = \vec{\nabla}\cdot\vec{A} = \frac{1}{h_1 h_2 h_3}\left[\frac{\partial}{\partial u_1}\left(h_2 h_3 A_1\right) + \frac{\partial}{\partial u_2}\left(h_3 h_1 A_2\right) + \frac{\partial}{\partial u_3}\left(h_1 h_2 A_3\right)\right] \tag{2.19}$$

From A.10, this gives $h_1 = 1, h_2 = r$, and $h_1 = 1$ so that

$$B_r = -\frac{1}{r_p}\frac{\partial}{\partial z}\left(r_p A_\varphi\right) + \frac{1}{r_p}\frac{\partial}{\partial \varphi}\left(r_p A_\varphi\right) = -\frac{\partial A_\varphi}{\partial z}$$

$$B_\varphi = \frac{\partial}{\partial z}\left(rA_r\right) - \frac{\partial}{\partial r}\left(A_z\right) = 0 \tag{2.20}$$

$$B_z = -\frac{1}{r_p}\frac{\partial}{\partial \varphi}\left(A_r\right) + \frac{1}{r_p}\frac{\partial}{\partial r}\left(rA_\varphi\right) = \frac{1}{r_p}\frac{\partial}{\partial r}\left(r_p A_\varphi\right)$$

For the derivatives of **K** and **E**, we use the formulas

$$\frac{\partial K(k)}{\partial k} = \frac{E(k)}{k(1-k^2)} - \frac{K(k)}{k} \quad \text{and} \quad \frac{\partial E(k)}{\partial k} = \frac{E(k)}{k} - \frac{K(k)}{k} \tag{2.21}$$

From (2.20),

$$\frac{\partial k}{\partial z} = -\frac{zk^3}{4Rr_p} \quad \text{and} \quad \frac{\partial k}{\partial r_p} = \frac{k}{2r_p} - \frac{k^3}{4r_p} - \frac{k^3}{4R} \tag{2.22}$$

Carrying out the differentiation, collecting terms, and substituting for k give

$$\vec{B}_r(r_p, z_p, R) = \vec{a}_r \frac{\mu_0 I}{2\pi} \frac{z_p}{r_p \sqrt{(R+r_p)^2 + z_p^2}} \left[-K(k) + \frac{R^2 + r_p^2 + z_p^2}{(R-r_p)^2 + z_p^2} E(k) \right] \tag{2.23}$$

$$\vec{B}_z(r_p, z_p, R) = \vec{a}_z \frac{\mu_0 I}{2\pi} \frac{1}{\sqrt{(R+r_p)^2 + z_p^2}} \left[K(k) + \frac{R^2 - r_p^2 - z_p^2}{(R-r_p)^2 + z_p^2} E(k) \right] \tag{2.24}$$
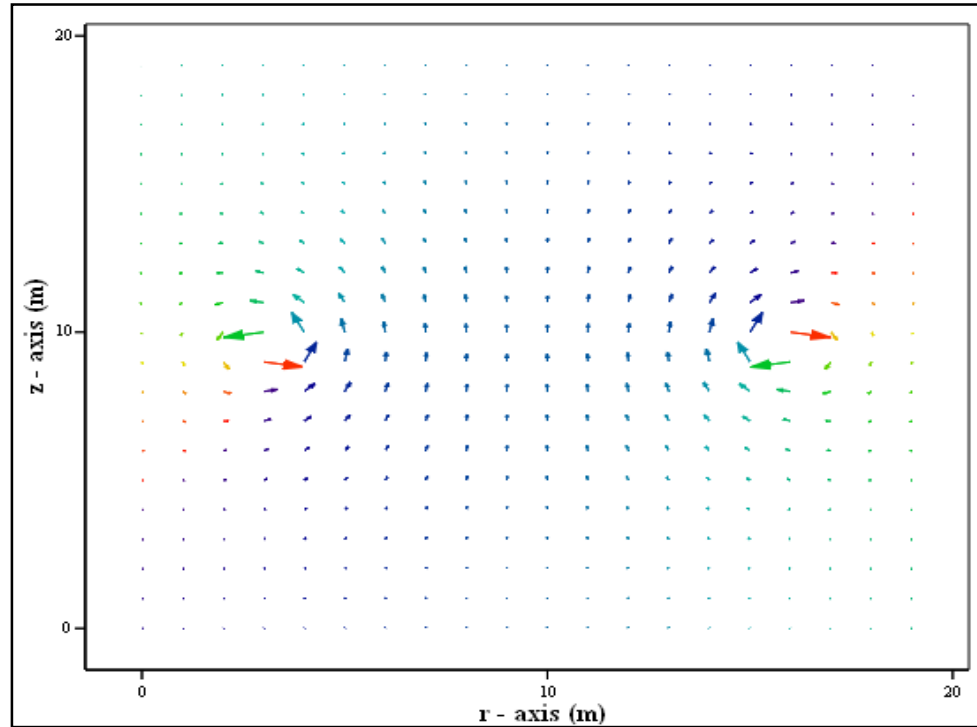
Figure 2.2. Cross section of magnetic flux density vector field through the circular loop

(I = 10 A, r = 4 m)
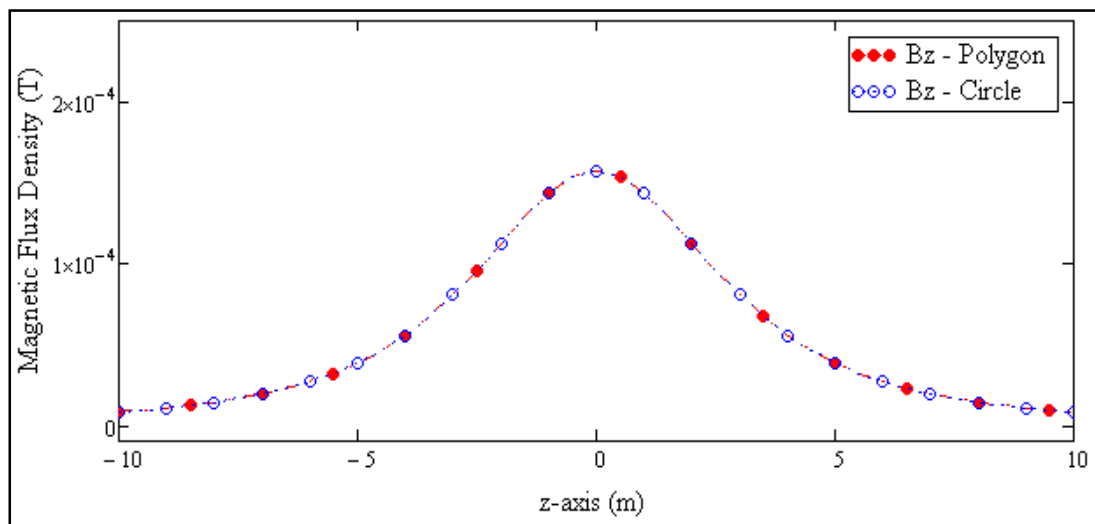
Figure 2.3. Comparison of polygon superposition method and circular loop elliptic integral

method for Bz values along z-axis (I = 1000 A, r = 4 m, Pn=60)
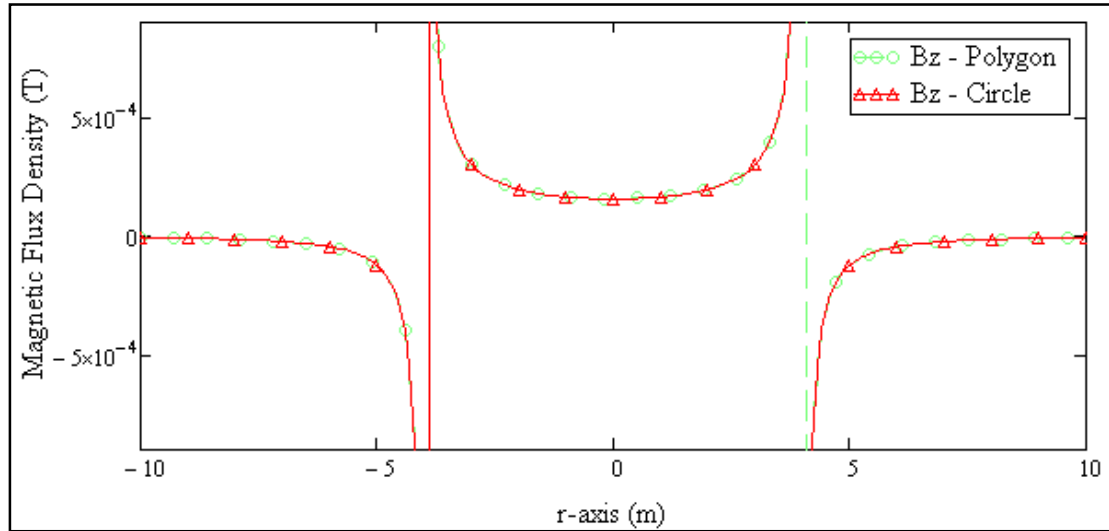
Figure 2.4. Comparison of polygon superposition method and circular loop elliptic integral method for Bz values along r-axis (I = 1000 A, r = 4 m, Pn=60)
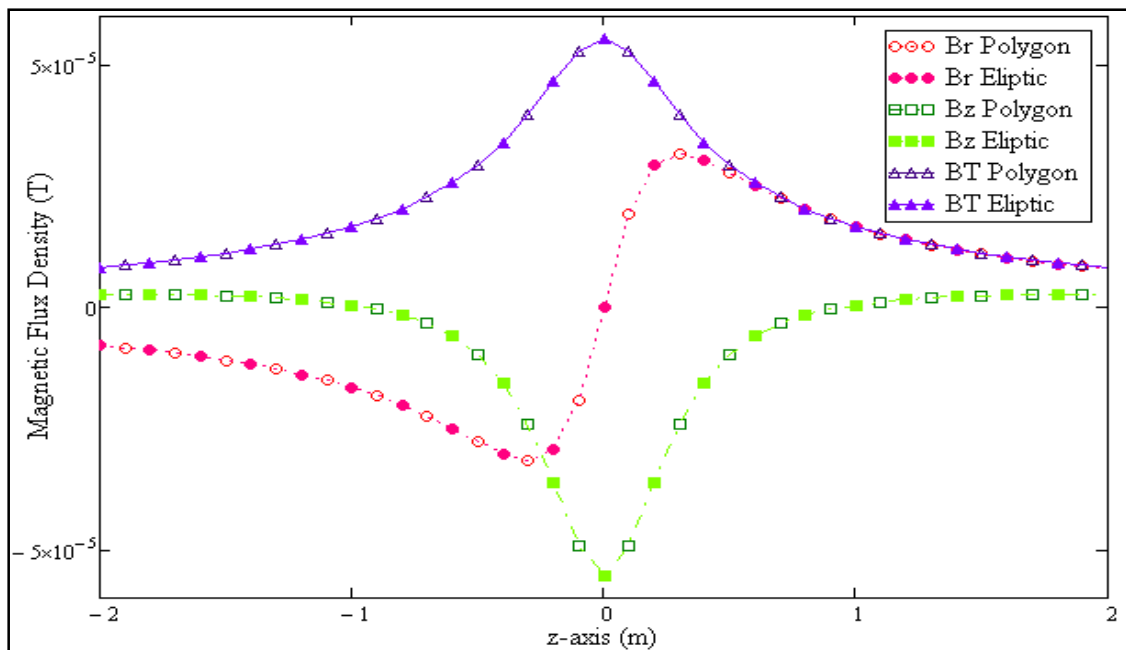
Figure 2.5. Comparison of polygon superposition method and circular loop elliptic integral method for Br, Bz, BT values of loop at r_p =4.3, φ_p =0, (I = 100 A, r = 4 m)

2.3. AC CHARACTERISTICS OF COIL

2.3.1. Estimating Resistance of Coil

The resistive losses in a solenoid are mainly from material conductivity, skin and proximity effects, radiation losses accounts small amount [12].

$$R_{total} = \Phi_M \Phi_{AC} R_{DC} + R_{radiation} \tag{2.25}$$

2.3.1.1. DC Resistance

DC resistance of a length of wire is due to the bulk resistivity of the material used and its conducting geometry. DC resistivity also changes with wire's diameter even though it is made up from same material. A table presenting the conductivity of copper with various wire diameters at $20^o C$ is presented in Appendix B. A generic formula for calculating resistivity is;

$$R_{DC} = \rho_{wire} \frac{length}{Area_{wire}} = \rho_{wire} \frac{length}{\pi \cdot radius^2} [\Omega] \tag{2.26}$$

The temperature on the wire has a scaling effect on the DC resistance. The relation of temperature effect is:

$$R_{T2} = R_{T1} \left(1 + \alpha \Delta T \right) \tag{2.27}$$

Where α is the temperature coefficient and for copper $\alpha_{copper} = 3.9 \cdot 10^{-3} [K^{-1}]$.

2.3.1.2. AC Resistance

When direct current is applied to a straight conductor it distributes itself evenly throughout the wire's cross-sectional area. When an alternating current is applied to a straight conductor, eddy currents develop and the current will tend to flow on the surface. As the AC

frequency is increased it becomes increasingly difficult for the current to penetrate into the center of the conductor, which flows along the conductor surface (skin). This increases the effective resistance of the wire and is called skin effect and is the major source of resistivity in a high frequency solenoid.

$$R_{AC} = \Phi_{AC} R_{DC} \tag{2.28}$$

Skin effect is essentially the inability of current to penetrate from the periphery toward the center of a conductor as the frequency is increased. This is a direct result of eddy currents established in the conductor from the changing AC flux (Figure 2.6). The eddy currents reinforce current flow on the conductor's "skin", decreasing exponentially as they move toward the center.

$$\delta(meters) = \frac{1}{\alpha} = \frac{1}{\text{Re}(\gamma)} = \frac{1}{\text{Re}\left(\sqrt{-\omega^2 \varepsilon \mu + j\omega\sigma\mu}\right)} \tag{2.29}$$

Direction of current flow
Unusable portion of conductor resulting from eddy currents
Eddy currents
Usable portion of conductor (skin)
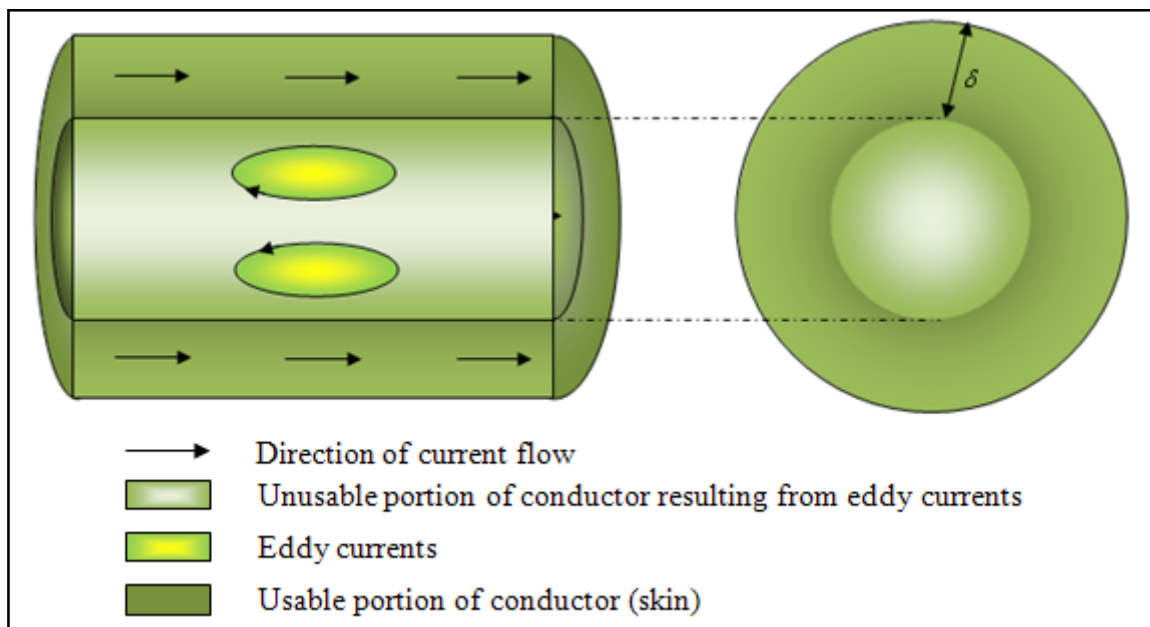
Figure 2.6. Illustration of eddy current (skin) effect on a wire

Where, δ is depth of current penetration from outer skin in meters, γ is the propagation constant, μ magnetic permeability of conductor, ε is electric permittivity of conductor and σ is conductivity of the conductor.

2.3.1.3. Proximity Effect

Proximity effects result from high-frequency current carrying conductors being in proximity to each other. While the proximity effect is dependent on the number of winding layers and layer construction, the skin effect is affected by the applied frequency. When a straight conductor is wound into a coil, the resulting proximity effects of the adjacent windings will produce even further losses.

$$R_{proximity} = \Phi_M R_{AC}$$ (2.30)
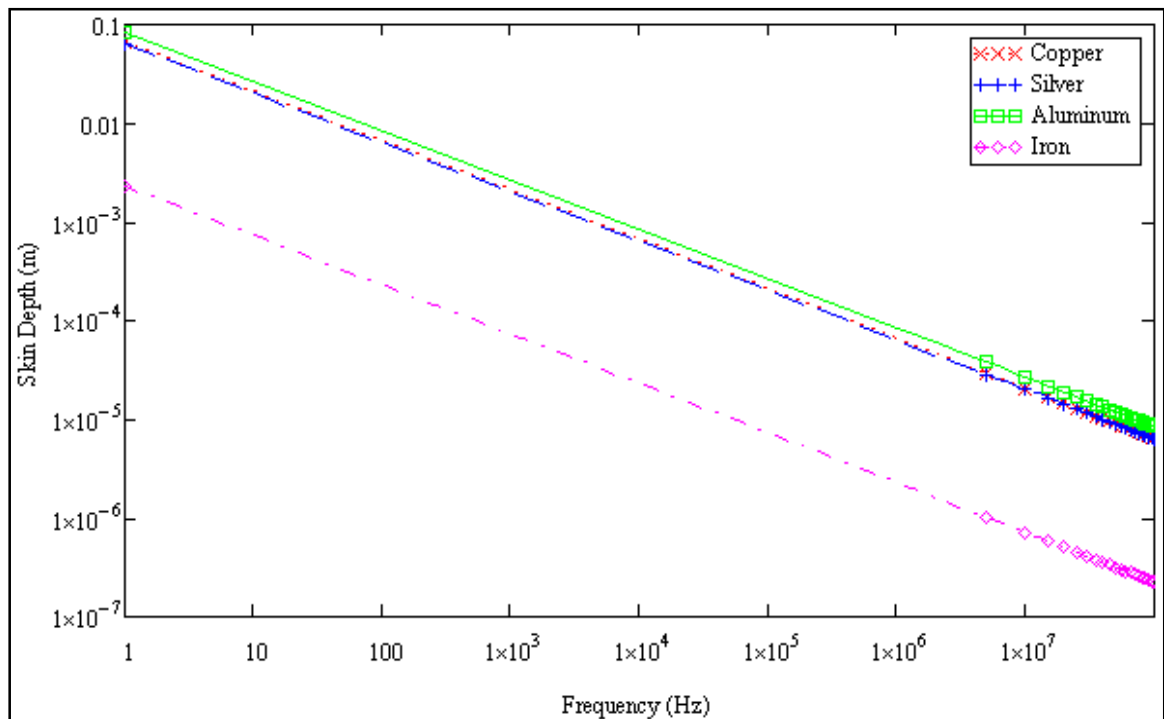
Figure 2.7. Skin depth versus frequency behavior of various conductors

2.3.1.4. Radiation Resistance

The radiation resistance increases when the coil structure radiates electromagnetic energy like an antenna. The radiation resistance is not strictly a measure of loss in the antenna but is analogous to the characteristic impedance, Z_0 of a transmission line [7].

$$R_{rad} = \sqrt{\frac{\mu_0}{\varepsilon_0}} \left[\frac{\pi}{12} N^2 \left(\frac{\omega R}{c} \right)^4 + \frac{2}{3\pi^3} \left(\frac{\omega R}{c} \right)^2 \right] \qquad (2.31)$$

2.3.2. Estimating Self Inductance of Coil

There are many numerical calculation methods and approximation in the literature. We present more accurate models below.

2.3.2.1. Long Solenoid Model

This model uses Ampere's law to derive inductance of a coil. It assumes that magnetic field inside the coil is constant. This assumption is reasonably true for the height of the solenoid approximately eight times greater than the radius, H>4R.

$$L_s = \frac{\mu_0 N^2 \pi R^2}{Height} [Henry] \qquad (2.32)$$

2.3.2.2. Wheeler's Formula

This method is the most common and practical one for calculating inductance of a uniform cylindrical solenoid. Wheeler's empirical formula is used primarily in designing RF and air core coils. It is useful in calculating inductances of short coils [13].

$$L_s = \frac{R^2 N^2}{9R + 10H} [\mu Henry] \qquad (2.33)$$

Where, R stands for radius in inches and H stands for height in inches. This formula gives good results for single layer wound solenoids and gives %5 accurate results for H>0.8 R.

2.3.2.3. Lundin's Formula

For comparison, Lundin's formula is the most accurate method of calculating inductance of a solenoid .It is derived from first principles and it is quite accurate.

$$L_s = \frac{\mu_0 N^2 \pi R^2}{H}\left[f(\frac{4R^2}{H^2}) - \frac{4}{3\pi}\frac{2R}{H} \right][Henry] \qquad (2.34)$$

$$f(x) = \frac{1 + 0.383901x + 0.017108x^2}{1 + 0.258952x}, \ 0 \le x \le 1 \qquad (2.35)$$

This formula is accurate up to three parts per million Henries; it is both nonlinear function of the coil's size and difficult to work with in equations when substituting an expression for inductance.   This formula gives much better prediction of induction than Wheeler's formula.

2.3.3. Estimating Self Capacitance of Coil

The proximity of windings in an inductor results in distributed capacitances. It can be imagined as series connected capacitors. Calculating distributed capacitances between the coil's windings and between the coil and ground requires detailed calculations using electromagnetic field equations.

2.3.3.1. Medhurst Capacitance Calculation

R.G. Medhurst, experimentally measured and published a table for estimating the effective capacitance, C_0, of a single layer solenoidal coil with mean radius R and height H. [14]

The capacitance is measured between the top winding of the coil and grounded bottom winding. This capacitance is assumed as capacitance between the coils windings and between the coil and the earth ground plane. Medhurst's formula is:

$$C_0 \approx 2Rh[pF] \qquad (2.36)$$

Where R is the radius of the solenoid in centimeters and h is a factor found from his experimental findings as shown in Table 3.1.

Table 3.1. Medhust Capacitance Table

$\dfrac{H}{2R}$	h	$\dfrac{H}{2R}$	h	$\dfrac{H}{2R}$	h
50	5.8	5.00	0.81	0.70	0.47
40	4.6	4.50	0.77	0.60	0.48
30	3.4	4.00	0.72	0.50	0.50
25	2.9	3.50	0.67	0.45	0.52
20	2.36	3.00	0.61	0.40	0.54
15	1.86	2.50	0.56	0.35	0.57
10	1.32	2.00	0.50	0.30	0.60
9.0	1.22	1.50	0.47	0.25	0.64
8.0	1.12	1.00	0.46	0.20	0.70
7.0	1.01	0.90	0.46	0.15	0.79
6.0	0.92	0.80	0.46	0.10	0.96

2.3.3.2. *Massarini, Grandi, Kazimierczuk Method*

An analytic derivation also presented by Massarini, Grandi, Kazimierczuk group in order to calculate single layer solenoid air core inductors for high frequency applications. [15]

$$C_0 = \frac{1}{N-1} \cdot \frac{\pi^2 2 R \varepsilon_0}{\ln\left[\frac{Di}{d} + \sqrt{\left(\frac{Di}{d}\right)^2 - 1}\right]} [pF]$$

(2.37)

Where N is the number of turns, Di is inter-winding gap, d is the wire diameter, R is the radius of solenoid.

2.3.4. Impedance and Reactance of a Coil System

Impedance of a coil can be modeled as series resistor and inductor by neglecting capacitive component. Application of AC signal to inductive element results in a lag of current and needs reactive power compensation. Inductive reactance component can be minimized by inserting series tuning capacitor in order to compensate current lagging. This reactive power compensation will result in full power transmission from oscillator to the pure resistive load, radiator. Similar wise receiver has to be power compensated in order to maximize reception of transferred inductive power. In Figure 2.8 series power compensation is presented.
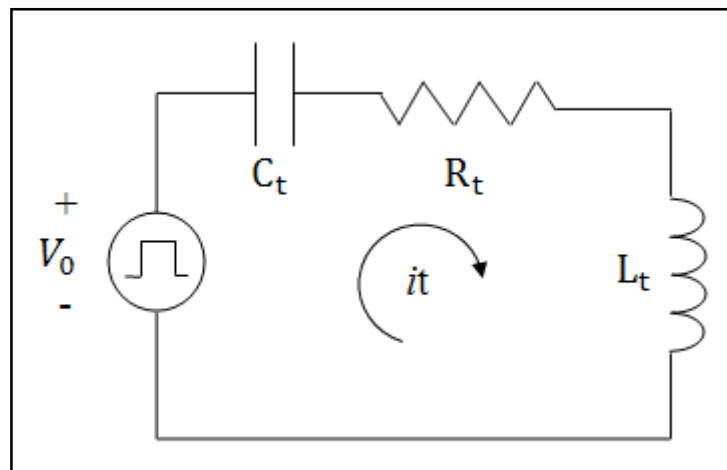
Figure 2.8. Series power compensation of an inductive radiator

Input impedance of a coil is presented in equation 2.38,

$$Z_{in} = R_{in} + jX_{in} = R_{DC+AC+Proximity} + R_{Radiation} + jwL_s + \frac{1}{jwC_s} \qquad (2.38)$$

At resonant frequency of a series RLC system, inductive reactance and capacitive reactance equalizes and results in pure resistive component. This allow oscillator to pump maximum power through this low resistive load.
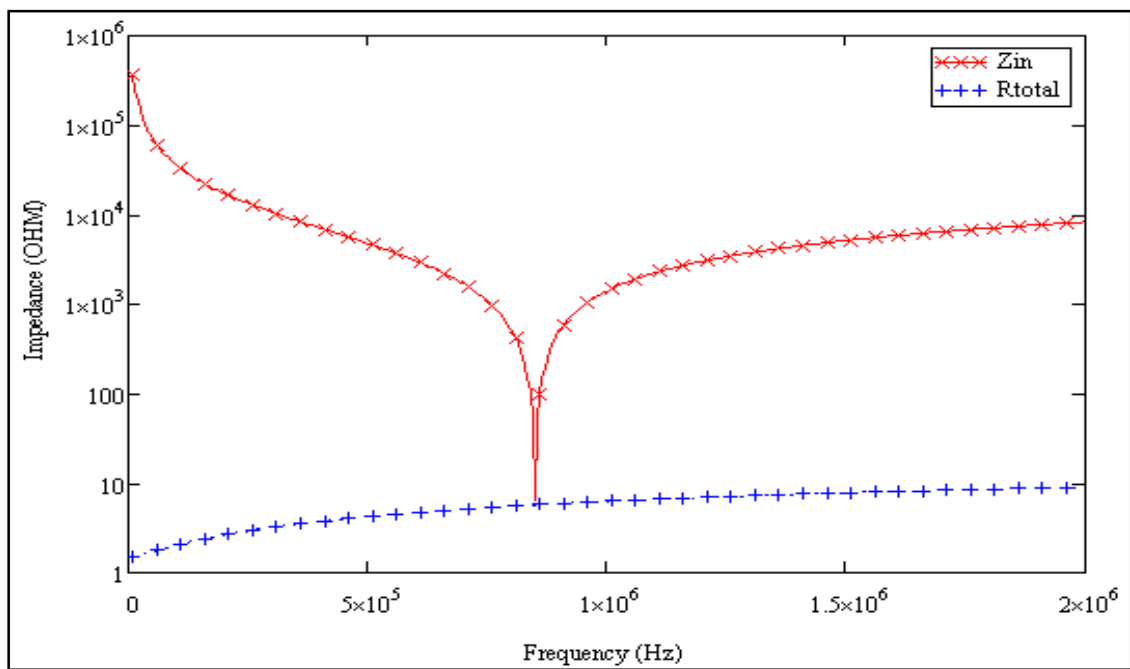
Figure 2.9. Impedance and total resistance versus frequency of a compensated radiator

As the frequency changes, input impedance becomes either inductive or capacitive reactive and results in increase of input impedance.
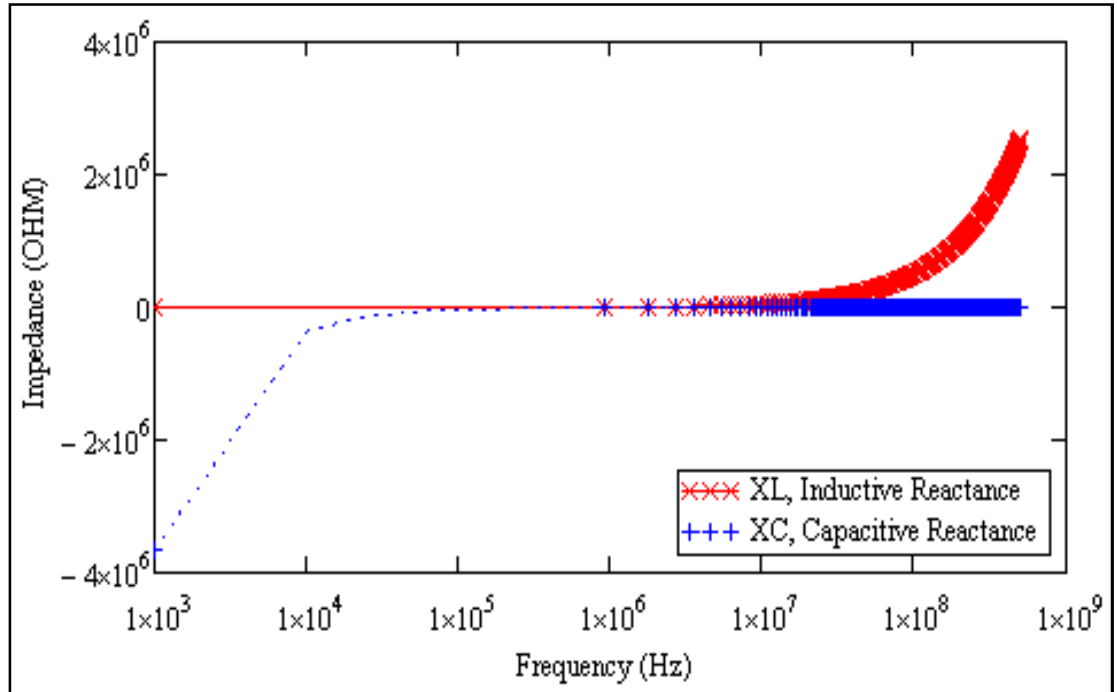
Figure 2.10. Inductive and capacitive reactance versus frequency
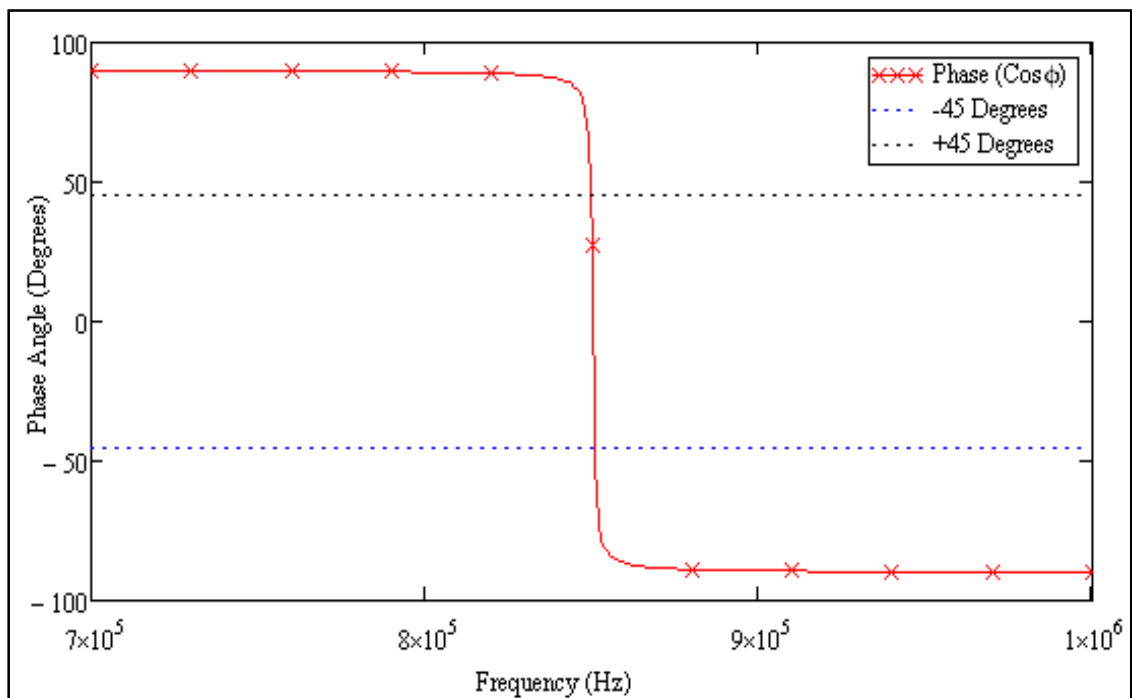
Figure 2.11. Current-Voltage Phase relationships at resonant frequency

Adding extra series capacitance will create lead in current and drive system to capacitive reactive state and system will have lower resonant frequency as shown in Figure 2.12.
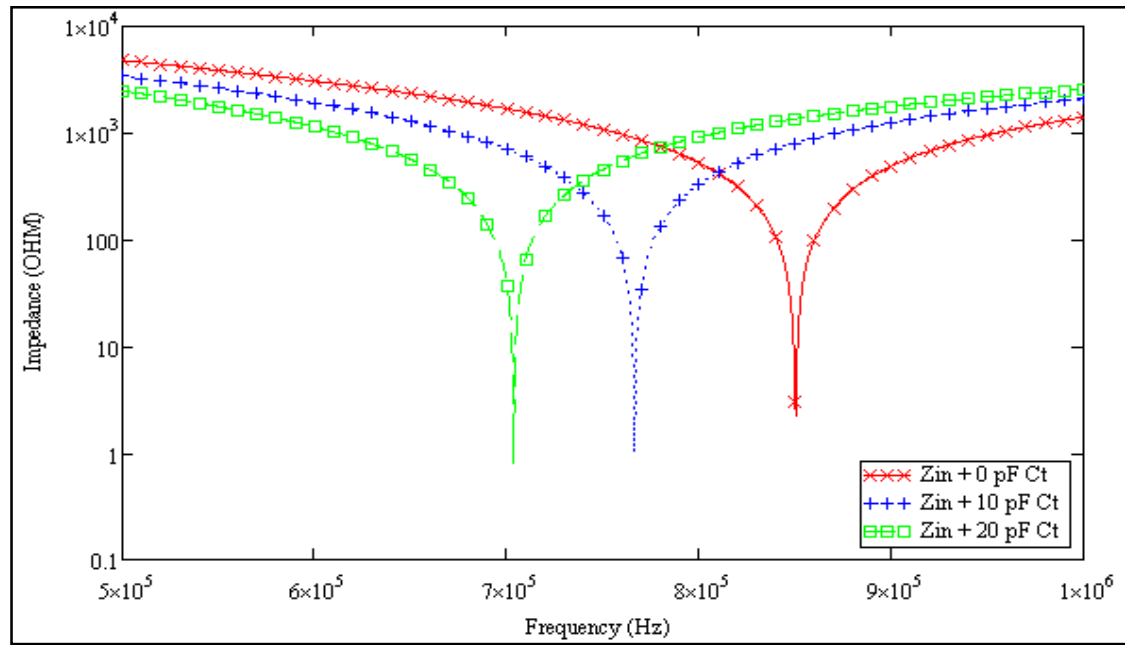
Figure 2.12. Effect of adding extra series capacitance

3. CIRCUIT MODEL OF WIRELESS POWER TRANSMISION

3.1. COUPLED NETWORK MODEL

A coupled resonant circuit is a pair of two circuits, each oscillating or resonating at one or more frequencies, mutually coupled by electromagnetic influences. These influences can be either electromagnetic, as observed in a transmitting antennae, inductive (magnetostatic), as in transformer, or capacitive (electrostatic). [16-20]

The coupled resonant circuit theory can be analyzed using second order RLC circuits and their mutual coupling to each other. Lumped element decomposition of system into generic elements such as resistances, inductances and capacitances makes analysis of the structure simple. The fundamental model of a coupled resonant system is shown in Figure 3.1.
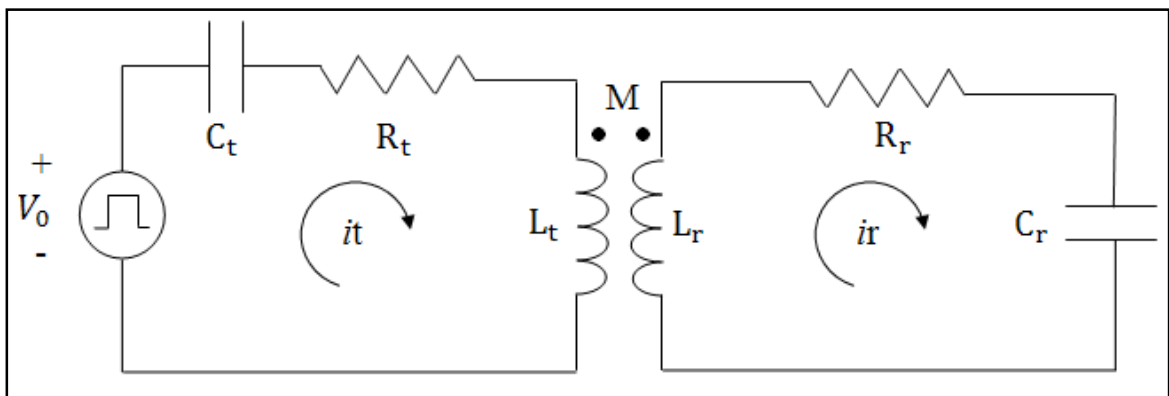
Figure 3.1. Lumped element (series RLC) model of resonant coupled circuit

This model shows two series circuits, comprised of a resistor, inductor, and capacitor (RLC), magneto-statically coupled by the mutual flux connecting their two inductors. The designation of series versus parallel topology comes from the location of the loss mechanism (resistance) in the circuit relative to the energy storage elements (capacitors or inductors).

3.1.1. Lumped Parameter Analysis and Second Order RLC Circuits

This section consists of an analysis of the frequency domain responses of second order RLC circuits and expressions to analyze maximum power transmission. There are general methods of analyzing second order circuits that allow tailored system responses to fit design criteria. One method is to introduce a generic frequency representation that can be adapted to fit both the series and parallel RLC cases, the Laplace transform.

The damping coefficient (ξ) representation is one of the most common methods used to represent second order response formulations. The representation comes from the second order differential equation shown in equation 3.1.

$$\frac{d^2 f}{dt^2} + 2\xi\omega_n \frac{df}{dt} + \omega_n^2 f = D(t) \tag{3.1}$$

The variables and parameters used in equation 3.1 are as follows: f is the function that describes a waveform in the second order system. It could represent a voltage or current as a function of time. The parameter ξ (unit-less) is the damping coefficient. Its value is an indication of the energy lost in the system per cycle of oscillation. It is used to calculate other parameters that describe features of the second order response. The frequency ω_n (rad/sec) is the characteristic resonant frequency of the system, the frequency at which the system would oscillate if uncoupled or undisturbed from any external influences. The term $D(t)$ is the driving force that couples the system to an external influence. This force can take the form of an input voltage or current.

The Q or Quality factor representation more directly relates to coil design requirements and is considered more useful in describing coil behavior. Q represents the ratio of the energy stored in the system divided by the energy lost per cycle. For a second order series RLC circuit, Q can be related to the ratio of circuit impedances: Z_L / R_{total}, the ratio of inductive impedance relative to total resistive loss, at the system resonant frequency, ω_n. The

conversion between Q and ξ is $Q = 1/2\xi$. As Q goes to infinity, the damped oscillation frequency approaches ideal resonant frequency, ω_n.

$$Q = \omega_n \frac{\text{(avarage energy stored)}}{\text{(energy loss / second)}} = \omega_n \frac{W_{magnetic} + W_{electric}}{P_{loss}} \qquad (3.2)$$

At ideal resonant frequency ω_n, magnetic stored energy and electric stored energy is equal. In order to maximize Q, P_{loss} needs to be minimized and $W_{magnetic} + W_{electric}$ needs to be maximized.

$$W_{magnetic} = \frac{1}{4}|I|^2 L, \quad W_{electric} = \frac{1}{4}|I|^2 \frac{1}{\omega^2 C}, \quad P_{loss} = \frac{1}{4}|I|^2 R \qquad (3.3)$$

From equation 3.2, Q factor can be derived as in equation 3.4 for series resonant coupled circuits,

$$Q = \omega \frac{\frac{1}{4}|I|^2 L + \frac{1}{4}|I|^2 \frac{1}{\omega^2 C}}{\frac{1}{4}|I|^2 R} = \omega \frac{L + \frac{1}{\omega^2 C}}{R} \qquad (3.4)$$

3.1.2. Coupled Resonant RLC Networks

Any circuit with two or more energy storage devices is called a resonating network. For the second order RLC circuit, there are two storage devices: a capacitor and an inductor. These two energy storage devices give the circuit, regardless of its topology, a single resonant frequency. Circuits with multiple pairs of energy storage elements have multiple resonant frequencies. These frequencies represent the speed of energy transfer between inductors and capacitors in the circuit. The power behind the lumped parameter model is that it takes a geometrically and spatially dependent system, containing distributed inductances and

capacitances and converts it into an electrical circuit model that can be analyzed with the tools of circuit theory.

When combining two second order circuits, each with its own resonant frequency and Q factor, the behavior of the total, fourth order system is not simply a sum, difference, or average of the two circuits. Different parts of the circuit resonate at different frequencies related to the original independent fundamental frequencies. As the system is driven by an external source, the energy it transfers to the circuit is moved between the energy storage elements of the circuit according to each device's constitutive relations. The result is that circuits will load one another and affect their natural resonance frequencies and individual Q factors.

3.1.3. Derivation of Dynamics in the Frequency Domain

A solution describing the operation of the coupled resonant system is presented below. The relationship between transmitter and receiver network helps us to understand the nature of the induced waveforms in the receiver.

We begin with derivation of series impedances as seen from the transmitter (Z_t) and receiver (Z_r) alone:

$$Z_t = R_t + j(\omega L_t - \frac{1}{\omega C_t})$$
(3.5)

$$Z_r = R_r + j(\omega L_r - \frac{1}{\omega C_r})$$
(3.6)

These impedances are defined for the circuit elements in series. Kirchhoff's rules are used on the circuit to derive system transfer function [13].

For a system driven by an input of the form $V_{in}(s)$, a transfer function $H(s)$ can be derived that relates the input, $V_{in}(s)$ to an output $V_{out}(s)$. The frequency domain variables are written in upper case letters. Kirchhoff's voltage equations are written for going around the transmitter and receiver circuits below:

$$V_{in} = I_t Z_t + j\omega M I_r \tag{3.7}$$

The equation 3.8 utilizes Faraday's and Lenz's laws to find the induced EMF in the circuit in the form of coupled inductance.

$$-j\omega M I_t = I_r Z_r \tag{3.8}$$

Solving equation 3.8 for I_s and then plugging it in the first equation to solve for I_p yields:

$$I_t = \frac{V_{in}}{Z_t + \dfrac{(\omega M)^2}{Z_r}} \tag{3.9}$$

$$I_r = \frac{-j\omega M I_t}{Z_r} = \frac{-j\omega M V_{in}}{Z_t Z_r + (\omega M)^2} \tag{3.10}$$

The effect of the receiver coupled to the transmitter is identical to that of additional impedance in the series path. Instead of the current in the transmitter being a simple voltage divided by its own impedance, there is an additional impedance of $(\omega M)^2 / Z_r$. This is due to the back EMF from the coupled receiver, with the sign according to Lenz's law. The receiver coil, having its own voltage produced by the transmitter, loads the transmitter in an effort to oppose the creation of magnetic flux in its inductor. This effect appears as a drop in the voltage around the transmitter circuit loop, acting as additional impedance.

The output voltage on the receiver coil, measured as the voltage across the capacitor is:

$$V_{out} = I_r \frac{1}{j\omega C_r} = \frac{-MV_{in}}{C_r \left(Z_t Z_r + (\omega M)^2 \right)} \tag{3.11}$$

$$\frac{V_{out}}{V_{in}} = \frac{-M}{C_r \left(\left(R_t + j\omega L_t + \frac{1}{j\omega C_t} \right) \left(R_r + j\omega L_r + \frac{1}{j\omega C_r} \right) + (j\omega M)^2 \right)} \tag{3.12}$$

Equation 3.12 is the transfer function, $H(j\omega)$, of the coupled second order series RLC resonant system.

$$M = k\sqrt{L_t L_r} \tag{3.13}$$

We place mutual inductance M, expand and order terms by their degree and present in s domain:

$$\frac{V_{out}}{V_{in}} = \frac{-k\sqrt{L_t L_r} C_t s^2}{\left\{ \begin{array}{l} (1-k^2)C_t C_r L_t L_r s^4 + (R_t L_r C_t C_r + R_r L_t C_t C_r)s^3 \\ +(R_t R_r C_t C_r + L_t C_t + L_r C_r)s^2 + (R_t C_t + R_r C_r)s + 1 \end{array} \right.} \tag{3.14}$$

The effect of coupling is actually adding impedance in series with transmitter RLC circuit. The magnitude of this coupled impedance is $Z_{coupled} = -(j\omega M)^2 / Z_r$, as derived in equation 3.9 and equation 3.10.
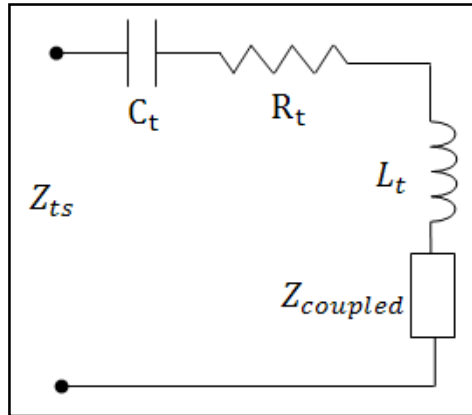
Figure 3.2. Schematic of equivalent transmitter circuit

$$Z_{tr} = Z_t + Z_{coupled} = Z_t + \frac{(\omega_t M)^2}{Z_r}$$

$$= R_t + jwL_t + \frac{1}{jwC_t} - \frac{(j\omega M)^2}{R_r + jwL_r + \frac{1}{jwC_r}} \tag{3.15}$$

The output impedance is more complicated to calculate in that the receiver capacitance is in parallel with the output terminals. The voltage induced on the receiver can be modeled as a voltage source supplying current to the receiver. Because of symmetry, the coupled impedance remains $Z_{coupled} = -(j\omega M)^2 / Z_t$. The output impedance is computed by finding the voltage across the capacitor in the receiver due to the induced voltage.

Using the expression for the receiver current derived in equation 3.10 and an induced voltage magnitude of $V_{induced} = -(j\omega M V_{in})/Z_t$ yields:

$$I_r = \frac{-j\omega M V_{in}}{Z_t Z_r + (\omega M)^2}, \qquad Z_{out} = \frac{V_{induced}}{I_r} \tag{3.16}$$

This can be expanded to give,

$$Z_{out} = \frac{\begin{cases} (M^2 - L_t L_r)C_t s^3 - C_t(R_t L_r + R_r L_t)s^2 \\ -(C_t R_t R_r + L_r)s - R_r \end{cases}}{\begin{cases} (M^2 - L_t L_r)C_t C_r s^4 - C_t C_r(R_t L_r + R_r L_t)s^3 \\ -(C_t(R_t R_r C_r + L_t) + L_r C_r)s^2 - (R_t C_t + R_r C_r)s - 1 \end{cases}} \tag{3.17}$$

Figure 3.3. Schematic of Equivalent Receiver Circuit Impedance

Output resistance is proportional to the characteristic impedance of a transmission line. Furthermore Z_{out} always has a resistive and capacitive component in series.

There is no physically consistent mathematical substitution for one of the parameters that will make it appear purely resistive or purely capacitive.

3.2. NONLINEAR DYNAMICS OF OSCILLATORS

Oscillators convert direct current (DC) power to radio frequency (RF). They are one of the most fundamental components in RF and microwave systems. However, an oscillator is inherently non-linear. If it were linear, the oscillation amplitude would grow indefinitely with time. [21, 22, 23] No steady state would be reached. For linear systems, the principle of superposition holds.

Oscillators are typically characterized as either L-C or R-C oscillators. We will work exclusively with L-C, or resonant, oscillators. L-C oscillators use a resonant circuit modeled by an inductor and capacitor to set the oscillation frequency. Depending on the frequency range, the resonant circuit is realized using a crystal (up to 500 MHz), dielectric transmission lines (500 MHz to 5 GHz), or dielectric resonators (2 to 40 GHz). The other major category of oscillator, the R-C type, is more commonly found in integrated circuits. Lacking inductors, R-C oscillators have much lower Q than L-C oscillators, and instead rely upon the charging and discharging of a capacitor to reach a threshold voltage that causes switching from one mode to another (as in the relaxation oscillator), or rely upon the propagation time delay and inversion through several devices to achieve a delayed output that can be fed back to the input (as in the ring oscillator). Although R-C oscillators are noisier than L-C oscillators, they can be tuned over much larger bandwidths (up to a decade), simply because the charging resistance can be implemented using an active device whose impedance can then be varied over a large range.

Ideally, an oscillator will generate an output current of the form,

$$i(t) = A\cos(\omega_0 t) = A\cos(2\pi f_0 t) \tag{3.18}$$

This is a pure sinusoid, represented by a single phasor of frequency f_0 in the frequency domain. In practice, both A and f_0 will fluctuate about their average values. The first fluctuation is amplitude noise and is generally lower in power than the second fluctuation, known as phase noise. Achieving the desired levels of A and f_0, minimizing the sources of phase noise, and tuning the frequency f_0 are the key oscillator design criteria

3.2.1. A Series Resonant Circuit as an Oscillator

We will take a simple circuit shown in Figure 3.4 to derive some fundamental expressions that are helpful in analyzing the behavior of an oscillator.
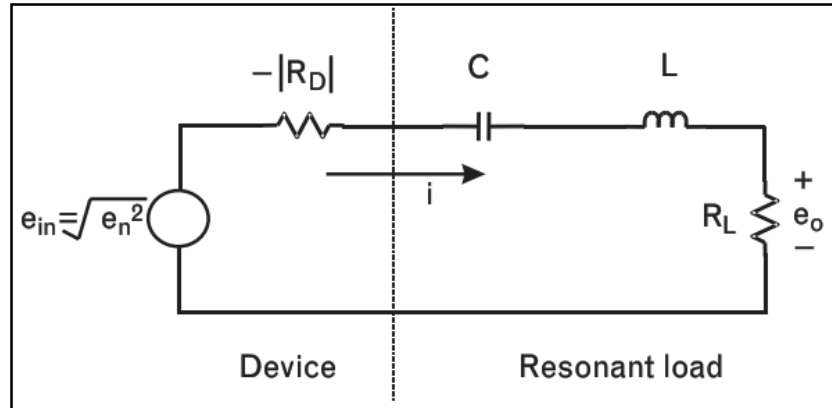
Figure 3.4. Series oscillator circuit, showing device resistance, resonant circuit, and load resistor

Assume that the excitation voltage in the Figure 3.4 is the bias voltage, which is switched on at t = 0. We can apply Kirchhoff's voltage law to the circuit to obtain;

$$e_{IN} = -|R_D|i + \frac{1}{C}\int_0^t idt + L\frac{di}{dt} + R_L i \qquad (3.19)$$

Or if we use the Laplace transform of the circuit and consider e_{IN} being step voltage;

$$\frac{e_{IN}}{s} = \left(R_L - |R_D|\right)i + \frac{i}{sC} + sLi \qquad (3.20)$$

The output voltage taken across RL may be written as iR_L or

$$e_o = \left(e_{IN}\frac{R_L}{L}\right)\frac{1}{s^2 + 2\xi\omega_0 s + \omega_0{}^2} \qquad (3.21)$$

Where,

$$\omega_0^2 = \frac{1}{LC},$$

(3.22a)

$$\xi = \frac{\left(R_L - |R_D|\right)}{2\omega_0 L} = \frac{1 - \left|\frac{R_D}{R_L}\right|}{2Q},$$

(3.22b)

$$Q = \frac{\omega_0 L}{R_L}$$

(3.22c)

The roots of equation 3.21 are given by,

$$s = \omega_0 \left(\xi \pm j\sqrt{1-\xi^2}\right)$$

(3.23)

So the inverse Laplace transform of equation 3.21 is given by,

$$e_o = \left(e_{IN} \frac{R_L}{L} \frac{1}{\omega_0 \sqrt{1-\xi^2}}\right) e^{-\xi\omega_0 t} \sin(\omega_0 t \sqrt{1-\xi^2})$$

(3.24)

Equation 3.24 is plotted in Figure 3.5 for both positive and negative values of ξ.
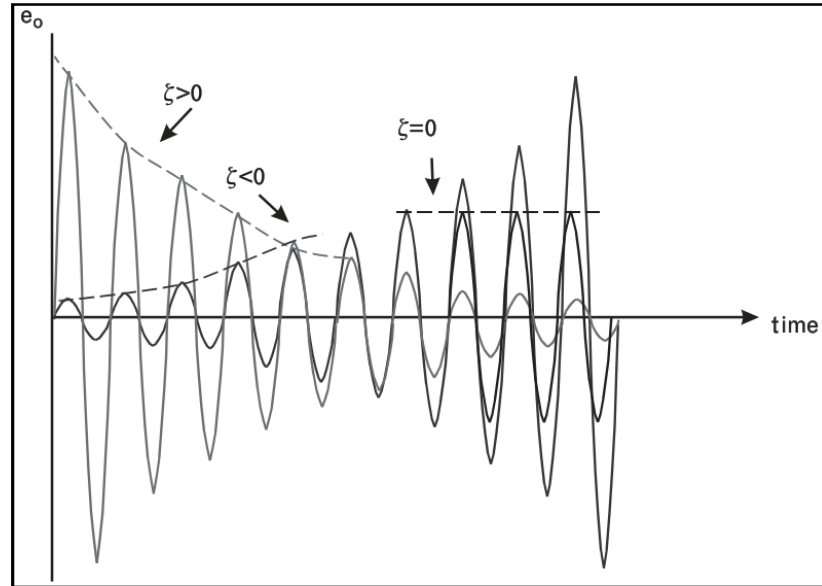
Figure 3.5. Output voltage of the series RLC circuit to a step response at the input

The time-domain response given by equation 3.24 is a sinusoid of frequency $\omega_0 \sqrt{1-\xi^2}$ multiplied by an envelope of value $e^{-\xi\omega_0 t}$. .The envelope can be written as $e^{-t/\tau}$, where τ is the time for oscillations to decay to $1/e$ of their initial value. The τ is equal to $1/\omega_0\xi$ so is directly proportional to Q. For positive values of ξ, the envelope decays over time and there is no steady-state oscillation. However, for negative values of ξ, oscillation grows exponentially because the envelope increases with time [24-27].

3.3. MUTUAL INDUCTANCES OF COILS

The mutual inductance (M) is affected by the proximity of the transmitter coil to the receiver and the geometries of both the transmitter and receiver. As the magnetic flux ($\vec{B}$) from the transmitter induces (couples) its magnetic field to the receiver, the magnetic field strength (H) in the receiver will have a higher density as it is moved closer to the transmitter and the more perpendicular the field is to the conductor (winding).

The basic building block of a cylindrical coil is the single turn or loop of wire. To evaluate the total inductance, self-inductance of a loop is first determined as a function of the wire diameter and the loop diameter. The coil consist of a number, N, of coaxial loops connected in series. The mutual inductances between all of the loops contribute to the total coil inductance. A general expression for the mutual inductance between two coaxial loops as a function of the mean diameters of the loops and the axial spacing is determined and this is used to calculate entire array of mutual inductance's between all of the coil's turns. In the general case the cross-section of the coil may be of any shape, rectangular, etc. The simplest case is the single layer solenoid. The method presented below is valid when all turns are coaxial. In general, the vector magnetic potential, $\vec{A}$, at a point r from a current element Ids is given by,

$$\vec{A} = \frac{\mu}{4\pi} \oint \frac{I\overline{ds}}{r}$$

(3.25)

The mutual inductance between two circuits, 1 and 2, is defined as the flux, Φ_{12}, through the circuit 1 due to a unit current in circuit 2, or vice versa. The flux of $\vec{B}\cdot\vec{n}$ field integrated over the area of any closed circuit is equal to the line integral of the magnetic vector potential around that circuit. The mutual inductance, M_{tr}, is therefore given by;

$$M_{tr} = M_{rt} = \int_{S_1} \overline{B_2} \cdot \overline{ndS_1} = \oint \overline{A_2} \cdot \overline{ds_1}$$

(3.26)

In principle, equation 3.26 can be applied to any two circuits to obtain the mutual inductance or to a single circuit to obtain self inductance.

The only component of the vector potential, A_φ, at point P on loop b due to a current in loop a is independent of φ. Here z and a1 are constant because of the coaxial location of the two loops.
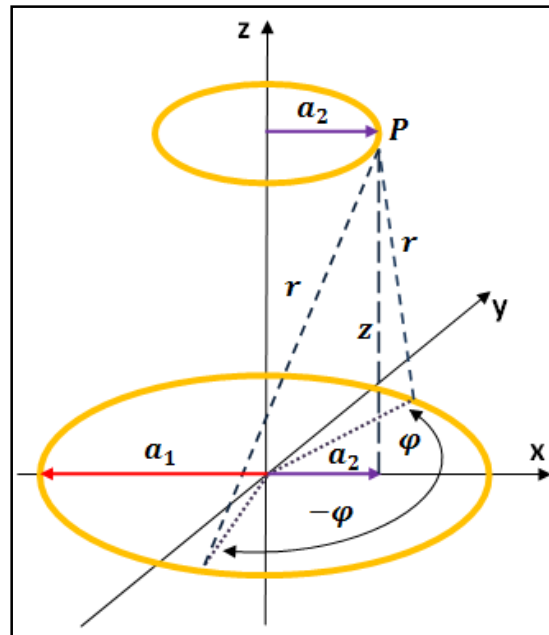
Figure 3.6. Mutual coupling between loops

It is assumed that current distribution is uniform on the current conductor and therefore current has symmetrical line location at the radius a_1. Under these conditions the vector potential at point P has only the component A_φ, and is given by;

$$A_\varphi = \frac{\mu I}{2\pi} \int_0^\pi \frac{a_1 \cos(\varphi) d\varphi}{\sqrt{a_1^2 + a_2^2 + z^2 - 2a_1 a_2 \cos(\varphi)}} \tag{3.27}$$

Since A_φ is the only component and is everywhere tangent to the loop radius a_2, then by equation 3.26, the mutual inductance M_{tr} between two loops of radii a_1 and a_2 axially spaced at z_{tr} is;

$$M_{tr} = \mu a_1 a_2 \int_0^\pi \frac{\cos(\varphi) d\varphi}{\sqrt{a_1^2 + a_2^2 + z_{12}^2 - 2a_1 a_2 \cos(\varphi)}} \tag{3.28}$$

3.3.1. Self Inductance of a Loop of Finite Size Wire

Figure 3.7 is the diagram of a loop of radius R made of wire with radius d and permeability μ' carrying a uniformly distributed total current I. The total self inductance can be determined by evaluating the B field energy within the wire plus the flux coupled to the inside diameter of the loop. The B field inside the wire is a function of the radius and is given by:

$$B(R) = \frac{\mu' R I}{2\pi d^2} \tag{3.29}$$

The total inductive energy stored in the wire is given by;

$$W_i = \frac{1}{2\mu'} \int_v B^2 dV = \frac{\mu' I^2 R}{8\pi^2 d^4} \int_0^d 2\pi R^3 dR = \frac{1}{2} L_{11} I^2 \tag{3.30}$$

The inductance component due to energy inside the wire is;

$$L_{11'} = \mu' \frac{R}{d} \tag{3.31}$$
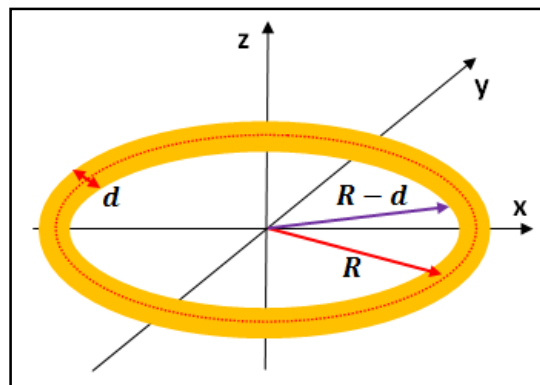
Figure 3.7. Loop radius illustration for magnetic flux calculations

The total flux external to the conductor, i.e., the total flux contained within radius R-d, is a measure of the inductance component external to the conductor. The flux is evaluated by equation 3.27. The vector potential component $A\varphi$ evaluated at radius R-d and $z=0$ and multiplied by the circumference, $2\pi(R-d)$, is the external flux by equation 3.26. Therefore the total inductance of the loop is given by;

$$L_o = \mu\frac{R}{4} + (\mu R(R-d))\int_0^\pi \frac{\cos(\varphi)d\varphi}{\sqrt{R^2 + (R-d)^2 - 2R(R-d)\cos(\varphi)}} \qquad (3.32)$$

3.3.2. Derivation of Co-Axial Coil Self Inductance
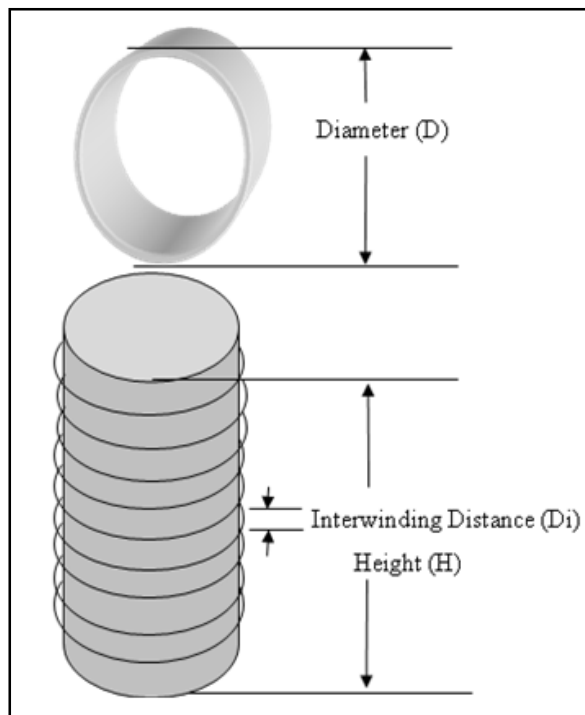
Figure 3.8. Coil with its design parameters

The general configuration of a co-axial coil is shown in Figure 3.8. The coil consist of N total coaxial loops, each having a specified wire radius, a loop mean radius, and axial position.

The axial position is only important in the determination of the relative axial positions of the N loops. The basic definition of inductance referred to two terminals is expressed as;

$$L_{1,2} = \frac{E_{1,2}}{\dfrac{di}{dt}} \tag{3.33}$$

Where; $E_{1,2}$ is the total voltage at terminals 1-2 as a result of the unit time rate of change of current passing through the terminals.

If we consider the general coil of Figure 3.8, the total voltage per unit rate of change of current consists of the total self inductance of the loops plus the sum of all of the mutual inductances.

Since $M_{v,w} = M_{w,v}$ each mutual will appear twice in determining the total voltage. Thus the total inductance of the coil is the sum of all of the elements in the inductance matrix as in equation 3.34.

The diagonal elements are the self inductances of the loops as determined by equation 3.32 and the symmetrical mutual inductances are determined by equation 3.34.

$$M_{v,w} = \sum_{1}^{N}\sum_{1}^{N} \begin{array}{cccc} L_1 & M_{1,2} & M_{1,n} & M_{1,N} \\ M_{1,2} & L_2 & M_{2,n} & M_{2,N} \\ M_{1,n} & M_{2,n} & L_n & M_{n,N} \\ M_{1,N} & M_{2,N} & M_{n,N} & L_N \end{array} \tag{3.34}$$

3.3.3. Mutual inductance of Coaxial Concentric Coils
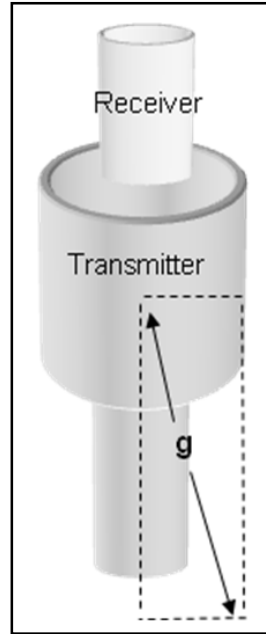
Figure 3.9. Coaxial concentric coil representation

$$M(\mu H) = 0.0501 \frac{R_r^2 N_t N_r}{g} \left[1 + \frac{R_t^2 R_r^2}{8g^4} \left(3 - 4 \frac{(0.5H_t)^2}{R_r^2} \right) \right] \tag{3.35}$$

Where, M is the mutual inductance of coaxial concentric transmitter and receiver coil in μH, Rr is the radius of receiver coil, Rt is the radius of transmitter coil, Nt is the number of transmitter coil turns, Nt is the number of receiver coil turns, Ht is the height of transmitter, g is the hypotenuse of imaginary right triangle formed from base of receiver coil and outer edge of the transmitter.

$$g = \sqrt{R_t^2 + (0.5H_r)^2} \tag{3.36}$$

Where, Hr is the height of receiver. The coefficient of coupling (k) can be calculated with the mutual inductance,

$$k = \frac{M}{\sqrt{L_t L_r}} \tag{3.37}$$

Where, k is coefficient of coupling between transmitter and receiver windings (less than1.0), M is mutual inductance of transmitter and receiver winding in μH, L_t is inductance of transmitter coil in μH, L_r is inductance of receiver coil in μH.

Table 3.2. Example transmitter and receiver coil parameters

Ambient temperature (TA) = 25 C	Transmitter Current = 10 A
Transmitter turns N1 = 13	Receiver turns N2 = 2440
Transmitter wire diameter d1 = 3.24 mm	Receiver wire diameter d2 = 0.324 mm
Transmitter Radius R2 = 22.86 cm	Receiver Radius R2 = 5.715 cm
Transmitter inter-winding gap di1 = 25.4 mm	Receiver inter-winding gap di2= 0 mm

We take parameters as in defined in Table 3.2 and have simulations for mutual inductance and coupling coefficient analysis for various parameter changes.
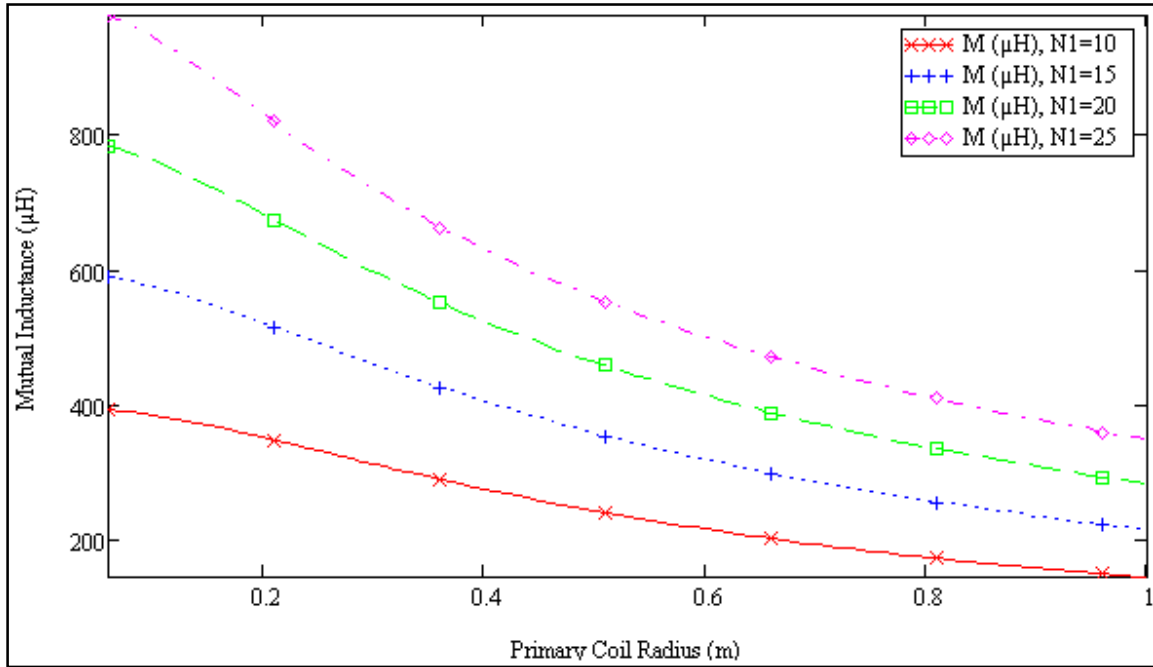
Figure 3.10. Mutual Inductance at Various Transmitter Radius and Turns
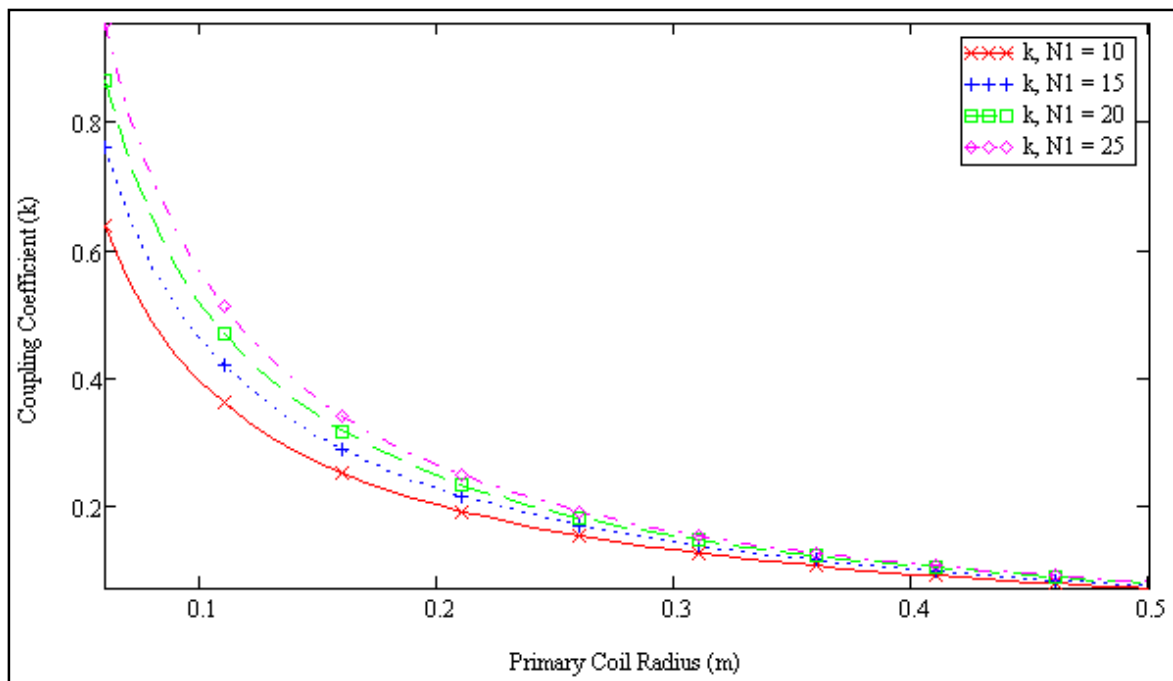
Figure 3.11. Coupling coefficient vs. transmitter radius with various turns
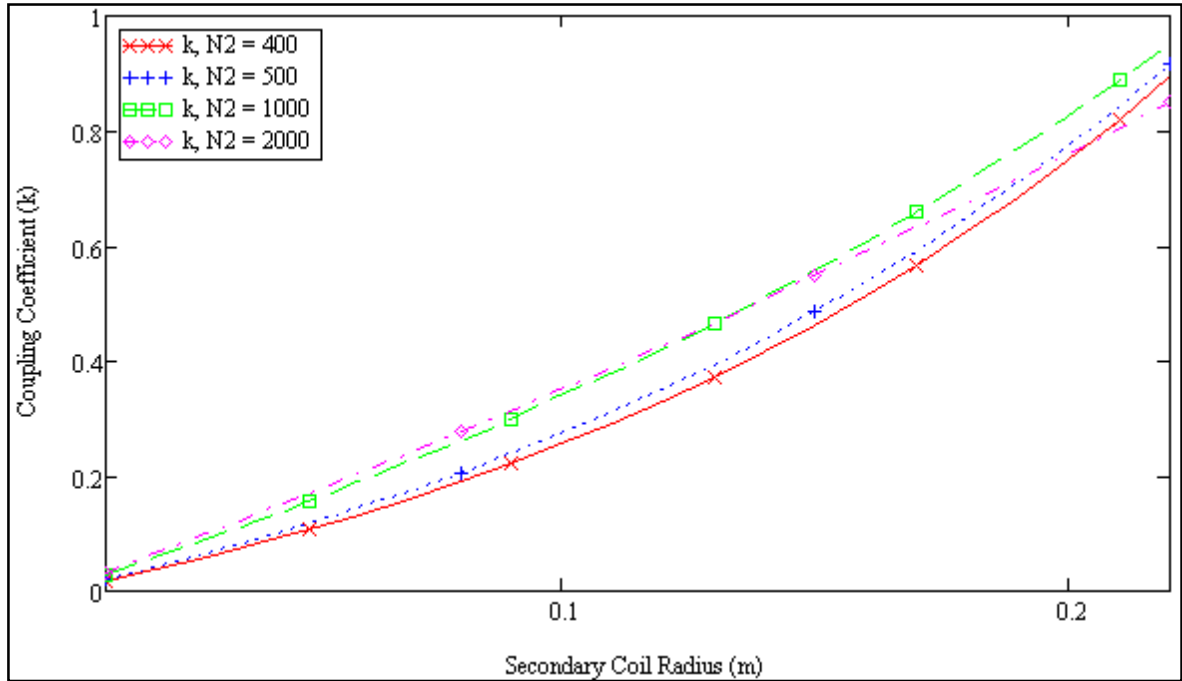
Figure 3.12. Coupling coefficient vs. various receiver radius and turns
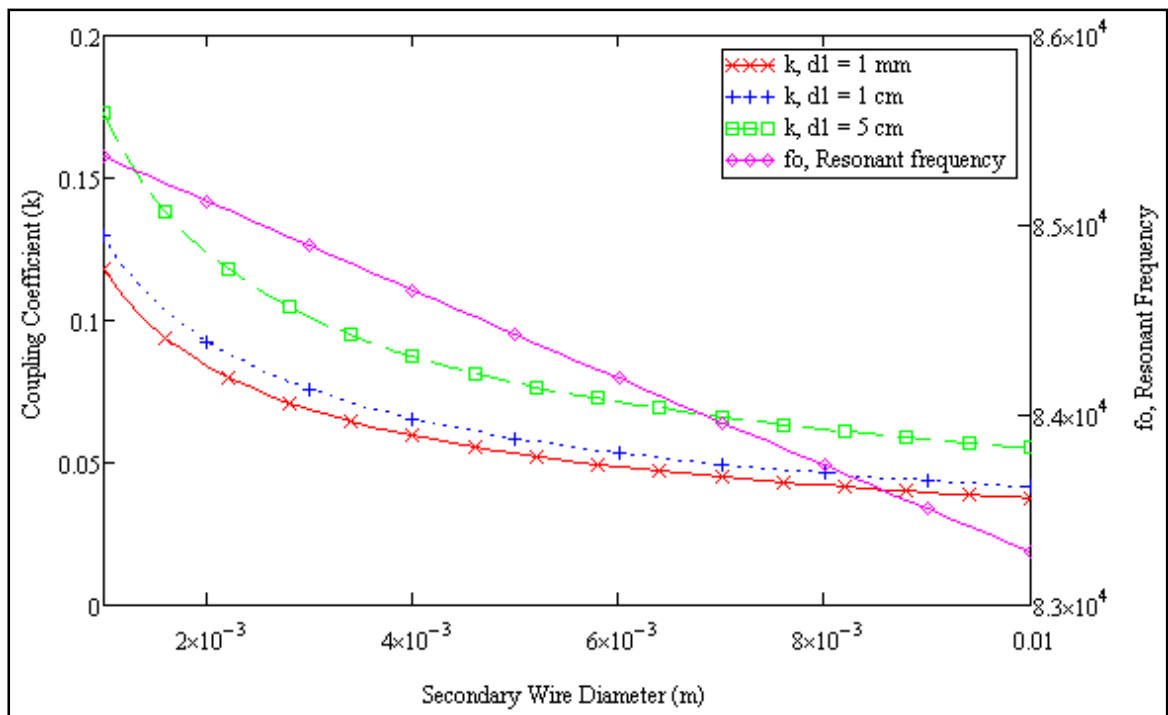
Figure 3.13. Coupling coefficient vs. various transmitter and receiver wire diameters
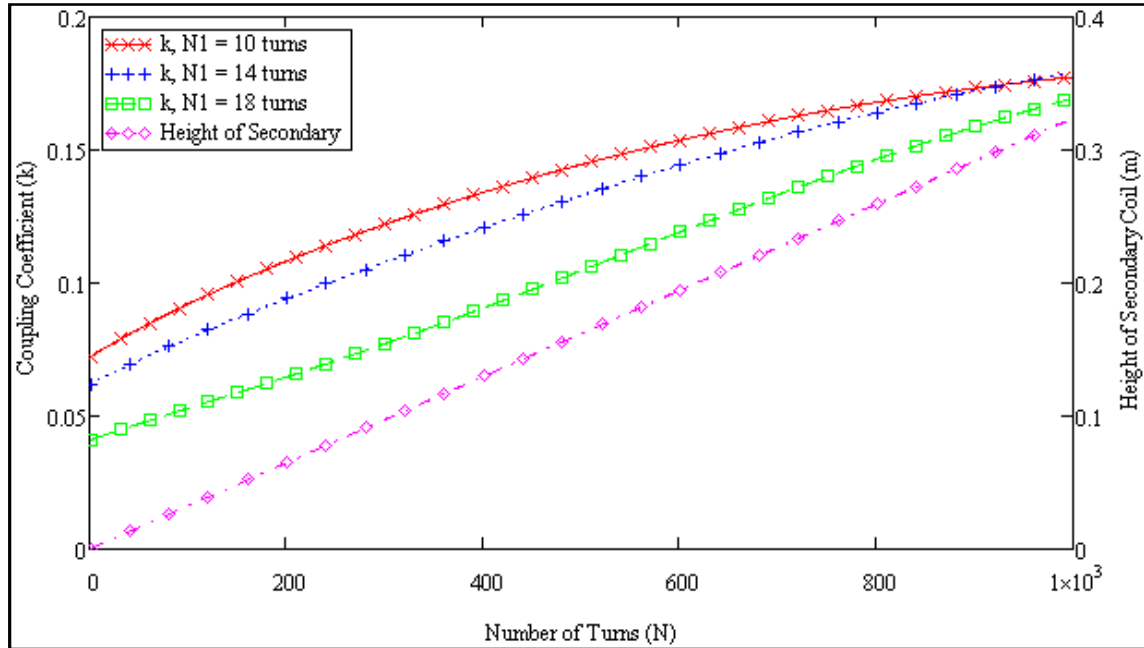
Figure 3.14. Coefficient coupling with various transmitter & receiver turns

3.3.4 Mutual inductance of Coaxial Non-concentric Coils
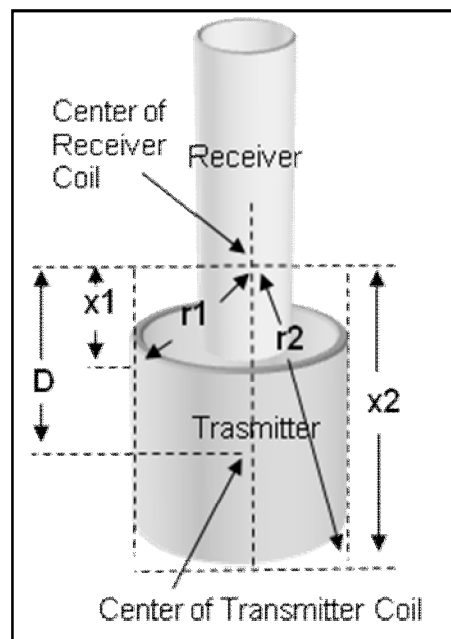
Figure 3.15. Coaxial non-concentric coil representation

$$M(\mu H) = 0.02505 \frac{R_s^2 R_p^2 N_p N_s}{4(0.5H_p 0.5H_s)} \left[K1k1 + K3k3 + K5k5 \right] \tag{3.38}$$

Where, M is mutual inductance of coaxial concentric transmitter and receiver winding in μH, Rr is radius of receiver coil, Rt is radius of transmitter coil, Nt is number of transmitter turns, Nt is number of receiver coil turns, Ht is height of transmitter, Hr is height of receiver. And the following form factors,

$$D = \left(0.5H_s - 0.5H_p \right) + Dsh \tag{3.39}$$

Where, Dsh is the separation from base of transmitter to base of receiver, k1 = Hr is the height of receiver

$$K1 = \frac{2}{R_p^2} \left(\frac{x2}{r2} - \frac{x1}{r1} \right) \tag{3.40}$$

Where, x1 is the distance from center of receiver coil to the upper edge of transmitter and calculated from x1 = D − (0.5Hp), x2 is the distance from center of the receiver coil to the lower edge of transmitter and calculated from x2 = D + (0.5Ht), r1 is the hypotenuse of imaginary right triangle formed from center of receiver coil and upper edge of the transmitter and calculated from $r1 = \sqrt{x1^2 + A^2}$, r2 is the hypotenuse of imaginary right triangle formed from center of receiver coil and lower edge of the transmitter and calculated from $r2 = \sqrt{x2^2 + A^2}$,

$$K3 = 0.5 \left(\frac{x1}{r1^5} - \frac{x2}{r2^5} \right) \tag{3.41}$$

$$k3 = R_s^2 0.5H_s \left(3 - \frac{4(0.5H_s)^2}{R_s^2} \right) \tag{3.42}$$

$$K5 = \frac{R_p^2}{8} \left(\frac{x1}{r1^9} \left(3 - \frac{4x1^2}{R_p^2} \right) - \frac{x2}{r2^9} \left(3 - \frac{4x2^2}{R_p^2} \right) \right) \tag{3.43}$$

$$k5 = R_s^4 0.5 H_s \left(\frac{5}{2} - 10 \frac{(0.5H_s)^2}{R_s^2} + 4 \frac{(0.5H_s)^2}{R_s^4} \right) \tag{3.44}$$
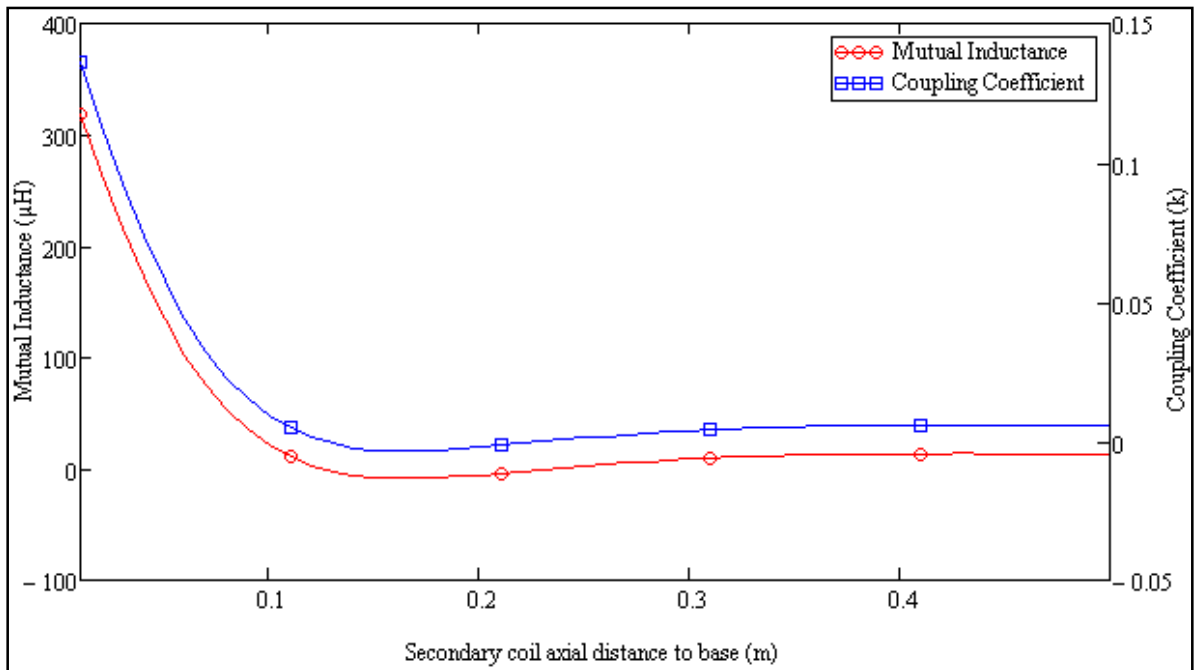
Figure 3.16. Mutual inductance and coupling coefficient while axially moving receiver out

3.3.5. Leakage Inductance Calculation

The mutual inductance is the degree of coupling the transmitter and receiver share. The leakage inductance is the inductance not shared between the transmitter and receiver. The mutual inductance couples the transmitter energy to the receiver. Since all the power must be accounted for (law of conservation), the power not transferred to the receiver is dissipated in the leakage inductance.

$$k = 1 - \left(\frac{Leakage}{L_t} \right) \qquad (3.45)$$

Where, k is the coefficient of coupling, leakage is measured leakage inductance of transmitter (magnetizing) winding in henries with receiver winding shorted together, Lt is inductance of transmitter (magnetizing) winding in henries.

The mutual inductance and coefficient of coupling affect the magnetizing inductance. Therefore the magnetic flux density (B) also depends on M and k. The magnetizing inductance is the inductance of the winding the current is being applied to (transmitter), the other winding in the transformer being the one the current is being transferred to (receiver). The magnetizing inductance is decreased by the coefficient of coupling:

$$L(h) = L_t (1 - k) \qquad (3.46)$$

Where, L is the inductance of transmitter (magnetizing) coil in henries, Lt is the inductance of transmitter coil in henries, k is the coefficient of coupling. Since k is always less than 1.0, the magnetizing inductance and B will always be less than that calculated without k. Higher k will result in lower magnetizing inductance.

4. ARRAY STRUCTURE FOR MAXIMUM POWER TRANSMISSION

4.1. POWER TRANSFER EFFICIENCY ANALYSIS

The efficiency of the coupled system depends on how much energy is transferred from the transmitter to the receiver circuit.

$$\eta_{energy} = \frac{E_{receiver,\max}}{E_{transmitter,\max}} \tag{4.1}$$

The maximum energy found on the transmitter, $E_{transmitter,\max}$, is the amount of energy initially put on the input capacitor C_t by the voltage source V_0.

$$E_{transmitter,\max} \approx E_{init} = \frac{1}{2}C_t V_{in}^2 \tag{4.2}$$

Where V_{in} is the voltage on C_t at time t=0, during positive pulse duration C_t acts like a voltage source and completes a series loop with the transmitter circuit elements, R_t, L_t and C_t
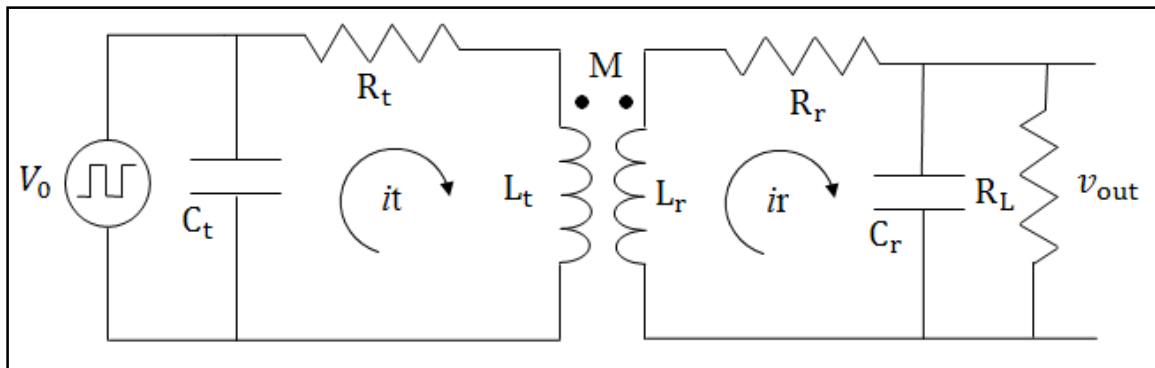
Figure 4.1. Resonant Wireless Power Transmission Lumped Circuit Diagram

The maximum energy transferred to the receiver is only a fraction of input energy. The energy found is receiver circuit is:

$$E_{receiver} = \frac{1}{2} L_r I_r^{\,2} + \frac{1}{2} C_r V_{C2}^{\,2}$$

(4.3)

The voltage across the receiver capacitor is defined to be the output voltage v_{out} of the coupled system. When this output voltage is at maximum, the energy in the capacitor is at maximum. When the energy stored in the capacitor is at maximum, the energy in the receiver can be assumed as maximum.

At maximum voltage level on receiver circuit, current becomes zero and no current flows from the circuit. At this point energy stored in receiver inductor is zero because current is zero. Thus, maximized receiver energy is:

$$E_{receiver,max} = \frac{1}{2} C_s V_{out,max}^{\,2}$$

(4.4)

To explicitly determine this maximum receiver energy, it is necessary to first determine the output voltage and its maximum value. The load R_L is connected across the receiver capacitance. The total output energy is defined to be the power dissipated by the load integrated over the lifetime of the output waveform. The output voltage across the load resistor is found by using the equivalent output impedance Z_{out} in a Thevenin equivalent circuit. Voltage across the load is:

$$v_{load}(t) = v_{out}(t) \left(\frac{R_{load}}{R_{load} + Z_{out}} \right)$$

(4.5)

To compute the energy delivered to the load, it is convenient to find the power delivered to the load;

$$P_{load} = \left(\frac{v_{out}}{R_{load} + Z_{out}} \right)^2 R_{load} \tag{4.6}$$

The power delivered to the load is maximized when the impedances are matched and purely resistive ($R_{load} = Z_{out}$). We derive peak receiver current using coupled circuit theory;

$$I_r = \frac{\omega_{ro} M I_t}{Z_r} \tag{4.7}$$

From current equation, we derive peak oscillating voltage on receiver,

$$V_r = -I_r \left(\frac{Z_r}{\sin(\omega_{ro} t_r + \delta S - \tan \phi S)} \right) \tag{4.8}$$

$$\tan \phi S = \frac{\omega_{ro}^2 L_r C_r - 1}{\omega_{ro} C_r Z_r} \tag{4.9}$$
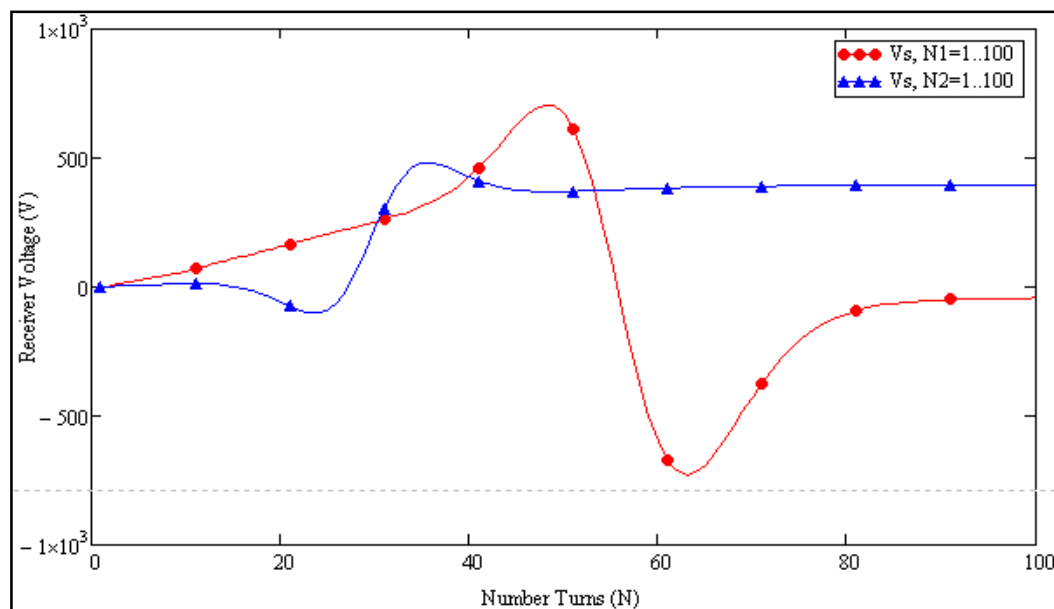
Figure 4.2. Receiver voltage and current while changing transmitter and receiver turns

We find power induced on receiver coil from:

$$P_r = \frac{\left(V_{r(rms)}\right)^2}{Z_r} \qquad (4.10)$$

And efficiency as a ratio of power received on receiver and transmitted power:

$$\eta = \frac{P_r}{P_t} \times 100 \qquad (4.11)$$
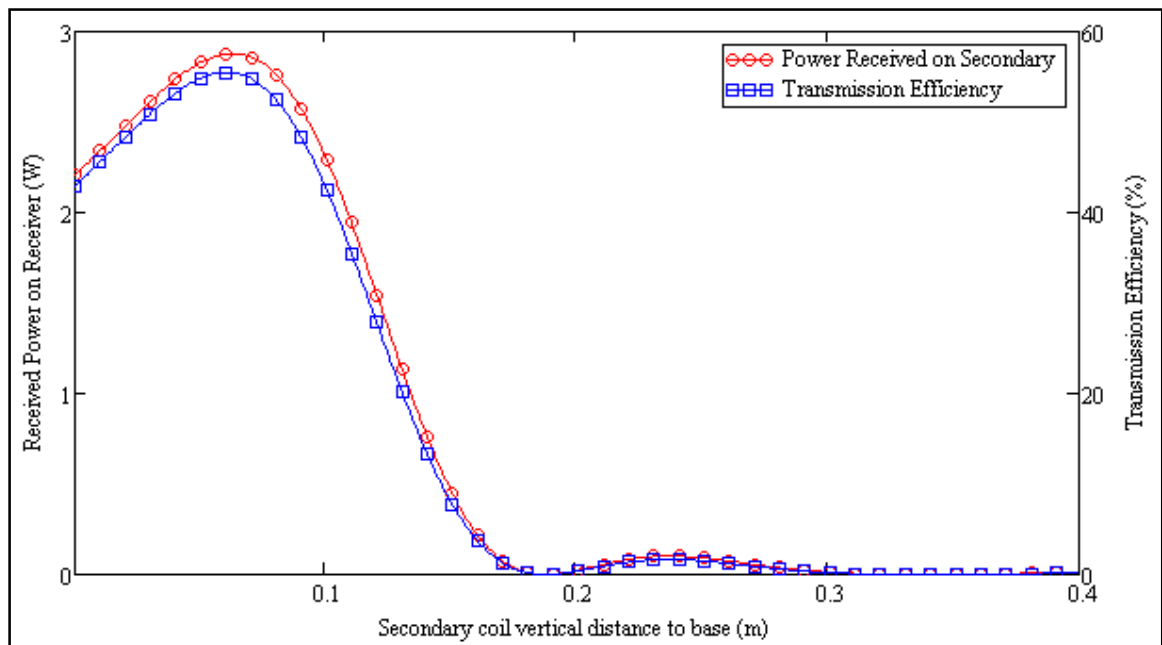
Figure 4.3. Received power on receiver while moving out of transmitter coil

As we remove receiver coil axially out of transmitter, we see exponential decrease on received power. Transmission efficiency is inversely proportional with the axial distance.

This is where the resonance comes in and helps efficiency dramatically by "tunneling" the magnetic field to a receiver coil that resonates at the same frequency. If resonant coupling

is used, where coils are tuned to a mutual frequency and the input current is modified from a sinusoidal into a non sinusoidal rectangular or transient waveform so as to more aggressively drive the resonance, significant power may be transmitted over a range of many meters.

Unlike the multiple-layer windings typical of non-resonant transformers, such transmitting and receiving coils are usually single layer solenoids or flat spirals with series capacitors, which in combination allow the receiving element to be tuned to the transmitter frequency and give low losses.

The tradeoff between high Q and bandwidth is a major problem with resonant coupling systems and needs to be analyzed deeper to utilize wider frequency spectrum. An array system with different resonant frequencies is presented in the next part in order to utilize wider spectrum as transmission medium.

4.2. MAXIMIZING TRANSMITTED POWER

In order to maximize transmission efficiency and transmitted power to the receiver, we need to maximize mutual inductance and coupling coefficient:

$$I_r = \frac{\omega_{so} M I_t}{Z_r} \qquad (4.12)$$

$$k = \frac{M}{\sqrt{L_t L_r}} \qquad (4.13)$$

Mutual coupling is directly related to geometrical design of the coils, i.e.: larger transmitter and receiver radius and higher transmitter and receiver turns increase mutual inductance while increasing the height of the coils decreases mutual inductance.

The ratio of the inductance L to the resistance R of a coil remains constant for different winding arrangements in the same volume and shape. It makes sense to define this value as a

figure of merit to distinguish different coil structures. The quality factor Q is defined by this ratio. The voltage, which is induced by the same current in an inductor scales with the frequency f and thus the apparent power in the device.

The general definition of the quality factor is based on the ratio of apparent power to the power losses in a device. From this definition, the quality factor of a coil results to:

$$Q = \omega \frac{(\text{avarage energy stored})}{(\text{energy loss / second})} = \omega \frac{W_{magnetic} + W_{electric}}{P_{loss}} = \frac{\omega L}{R} \qquad (4.14)$$

Increasing Q factor results in lower BW radiator and receivers. The tradeoff between bandwidth and Q factor, limits us to utilize small portion of spectrum while having high Q factor. In the next part, we propose an array structure approach to solve narrow band utilization.

4.3. MAXIMIZING TRANSMISSION SPECTRA

As indicated in Chapter 2, we limit ourselves to use a limited rectangular box space for the transmitter and receiver radiators.

Our approach to solve limited space power transmission is to maximize transmission spectra with array structured transmitter and receiver apertures. We know that high Q receivers tuned for a part of spectrum receive only related part of the spectrum (receiver's resonant frequency), so we design array transmitter system with separate resonant frequencies and receivers with exact couples of transmitters.

In order to simulate near field characteristics of transmitter and receiver coils, we have designed set of FEKO simulations based upon our Q factor calculations.

We first analyze broadband response of 10 MHz resonant transmitter and receiver couples with FEKO simulation software, then we analyze 5MHz transmitter and receiver couple. We compare FEKO results with our analytical calculations in MathCAD for comparison,

10 MHz coupled system parameters: Dsh (axial distance between coils) = 10 cm, N (number of turns) = 4, R (radius) = 4 cm, d (wire diameter) = 0.5 mm, Di (inter-winding distance) = 0.8 mm.
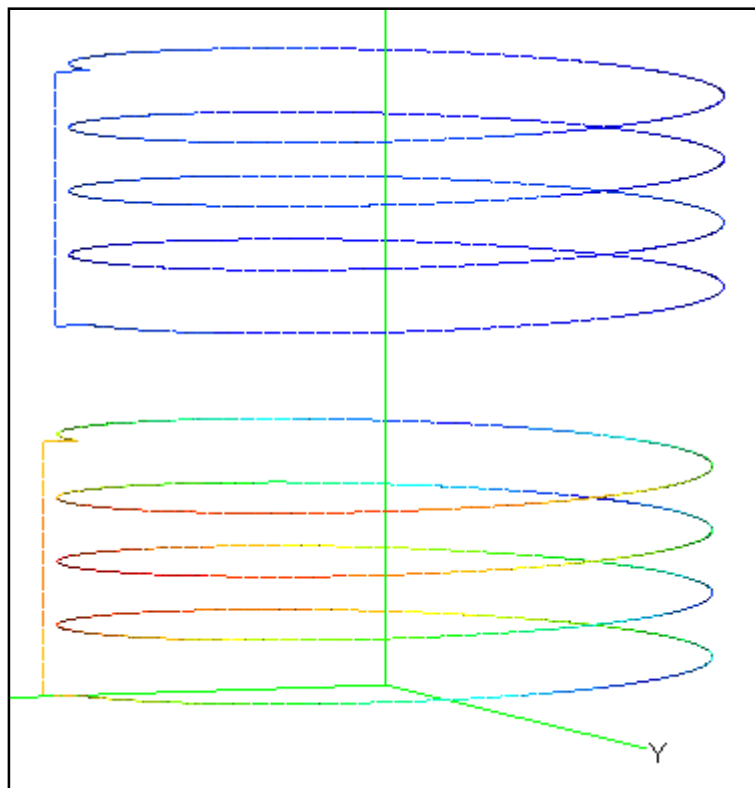
Figure 4.4. FEKO simulation of 10 MHz resonant transmitter and receiver coils.
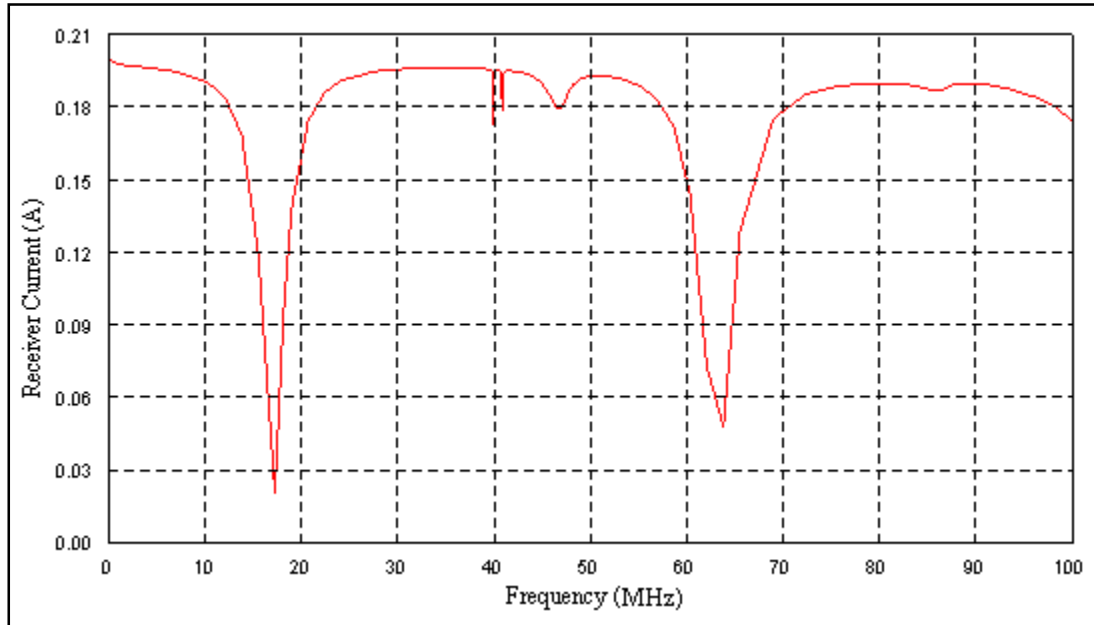
Figure 4.5. Wideband current response of transmitter coil with fo =10 MHz
Dsh = 13 cm, N = 4, R = 26.5 cm, d = 0.8 mm, Di = 2.5 cm (FEKO simulation)
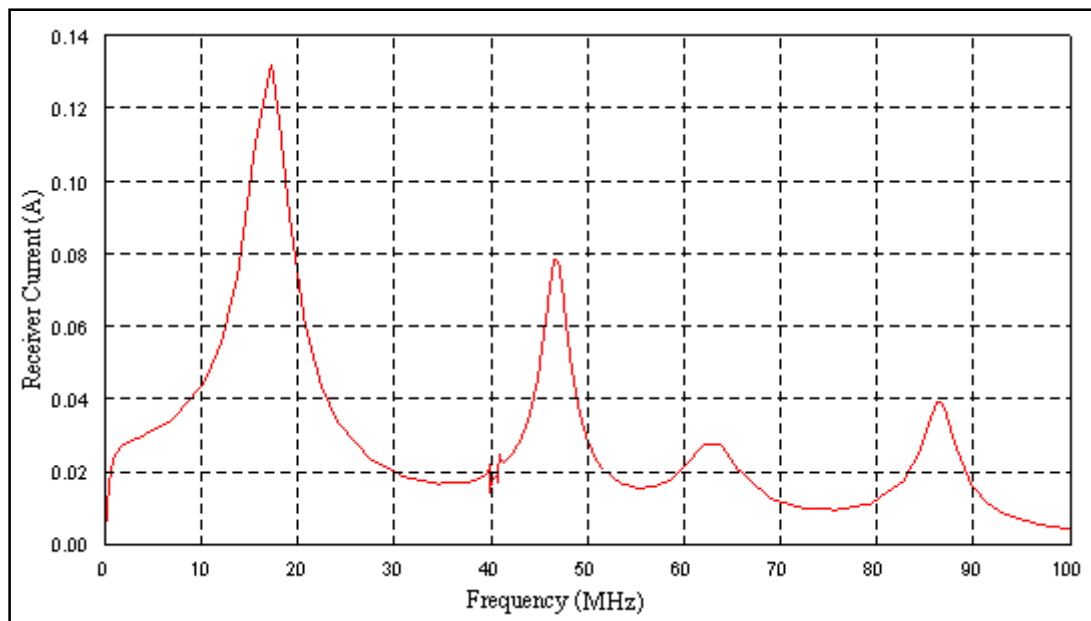
Figure 4.6. Wideband current response of receiver coil with fo =10 MHz
Dsh = 13 cm, N = 4, R = 26.5 cm, d = 0.8 mm, Di = 2.5 cm (FEKO simulation)
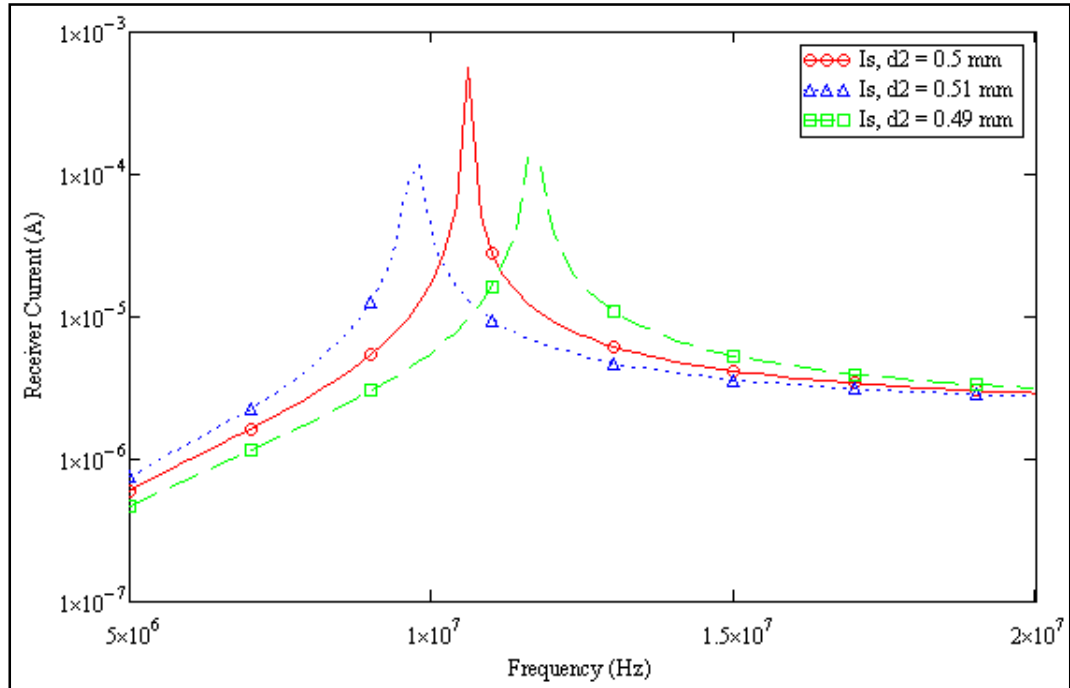
Figure 4.7. MathCAD simulation of receiver current near resonant frequency with various receiver wire diameters Dsh = 13 cm, N = 4, R = 26.5 cm, d = 0.8 mm, Di = 2.5 cm
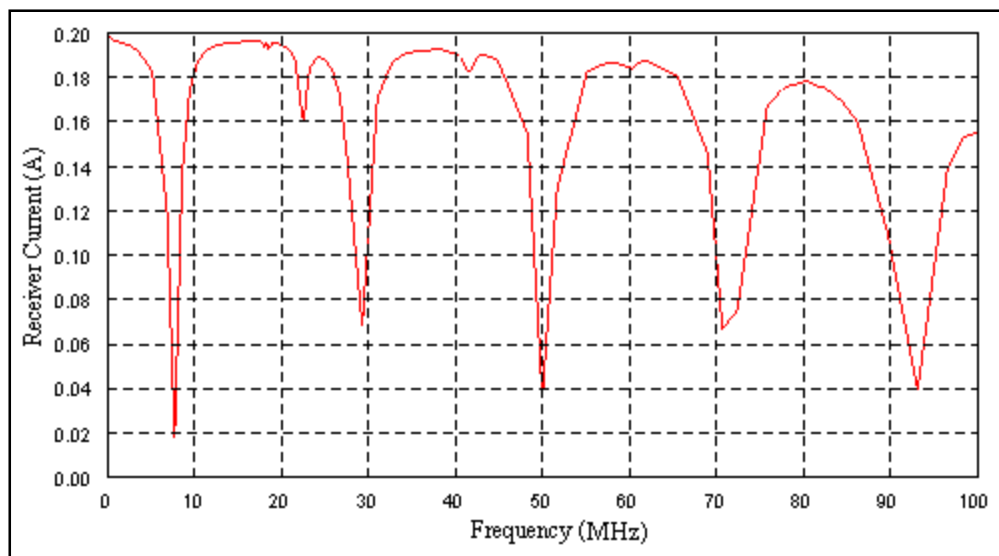
Figure 4.8. Wideband current response of transmitter coil with fo = 5 MHz
fo = 5 MHz, Dsh = 13 cm, N = 6, R = 38.1 cm, d = 0.8 mm, Di = 2.5 cm (FEKO Sim.)
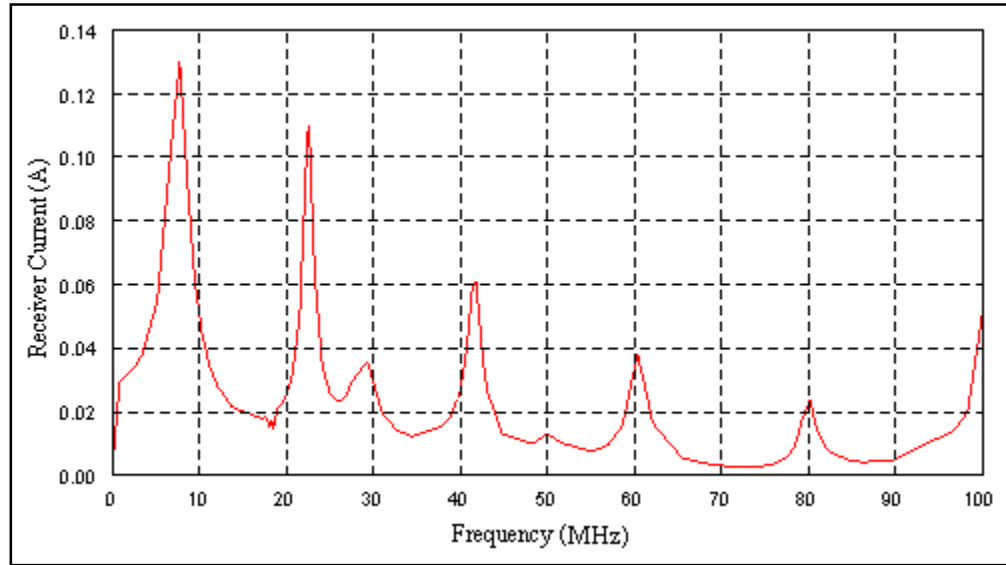
Figure 4.9. Wideband current response of receiver coil with fo =5 MHz

fo = 5 MHz, Dsh = 13 cm, N = 6, R = 38.1 cm, d = 0.8 mm, Di = 2.5 cm (FEKO Sim.)
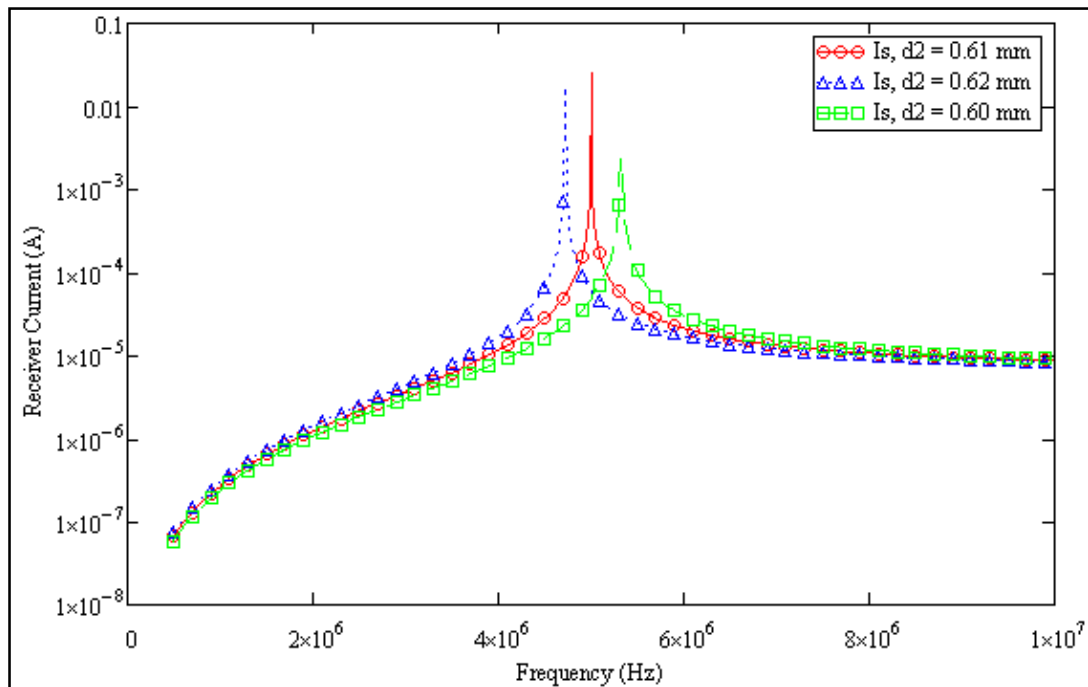
Figure 4.10. MathCAD simulation of receiver current near resonant frequency with various receiver wire diameters fo= 5 MHz, Dsh= 13 cm, N= 6, R = 38.1 cm, d = 0.8 mm, Di = 2.5 cm

Next, we analyze array transmitter and receiver system. We combine 10 MHz coupled system with 5 MHz coupled system. We find that each coupled circuit has small interference from the neighboring wireless transmission line.
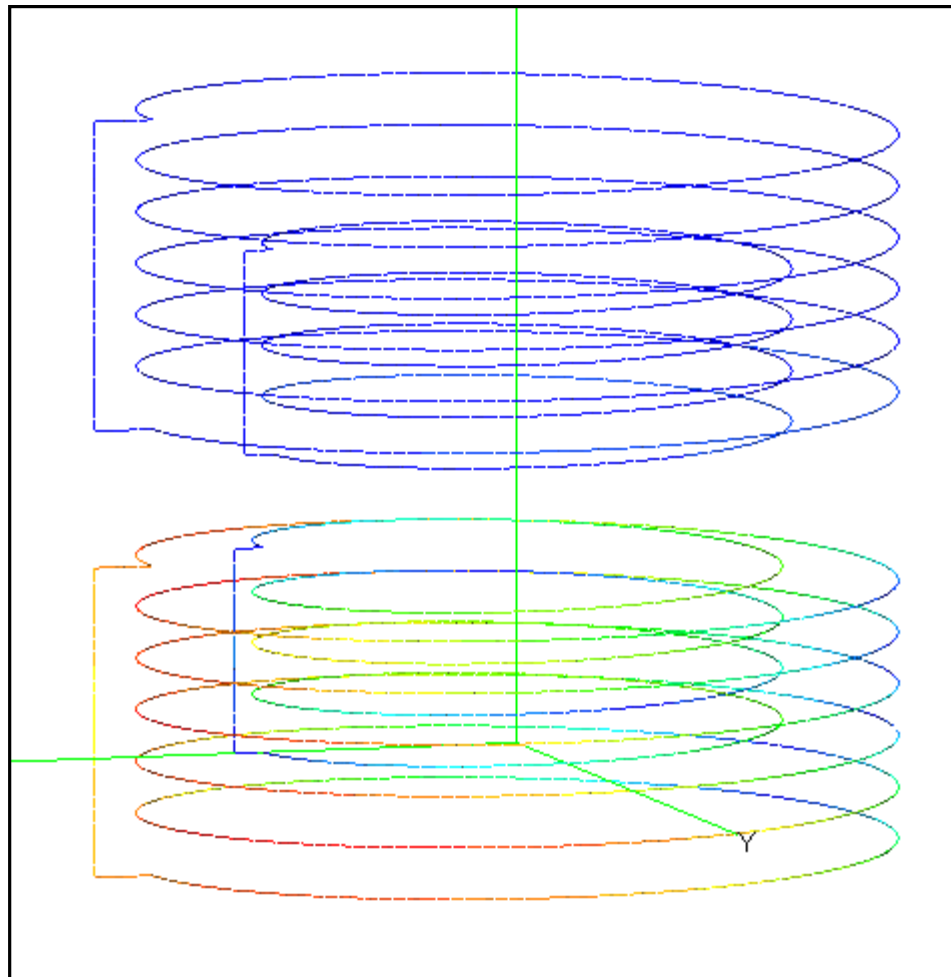
Figure 4.11. Dual transmitter and dual receiver

(10 MHz + 5 MHz transmitter and receiver) (FEKO simulation)
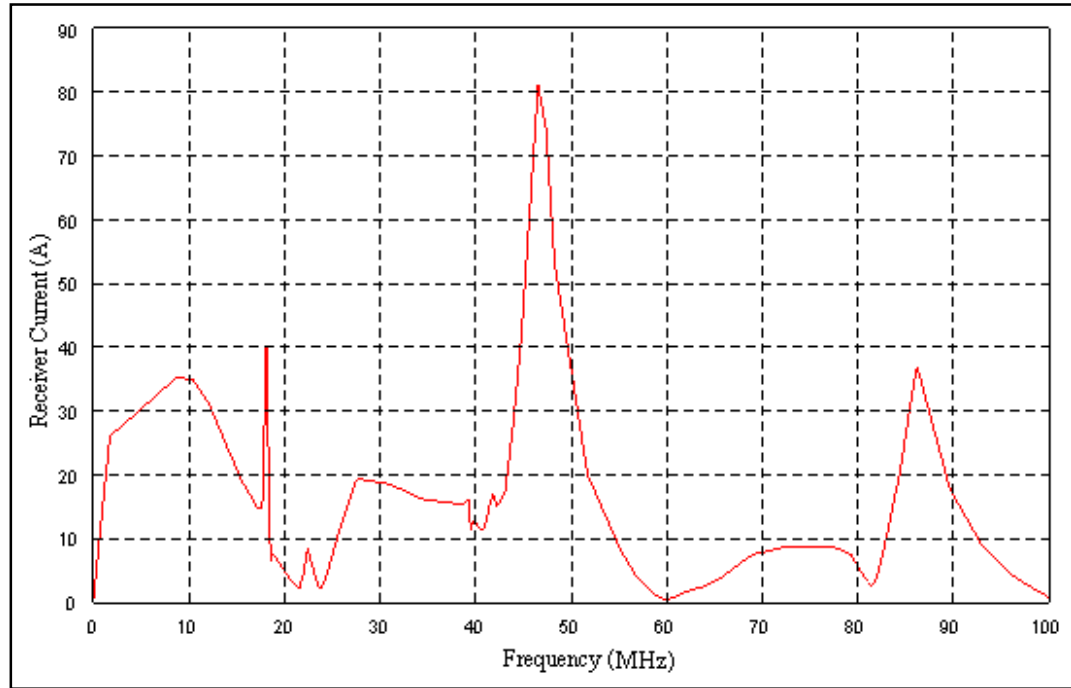
Figure 4.12. Wideband current response of transmitter coil with fo = 5 MHz (Array System)
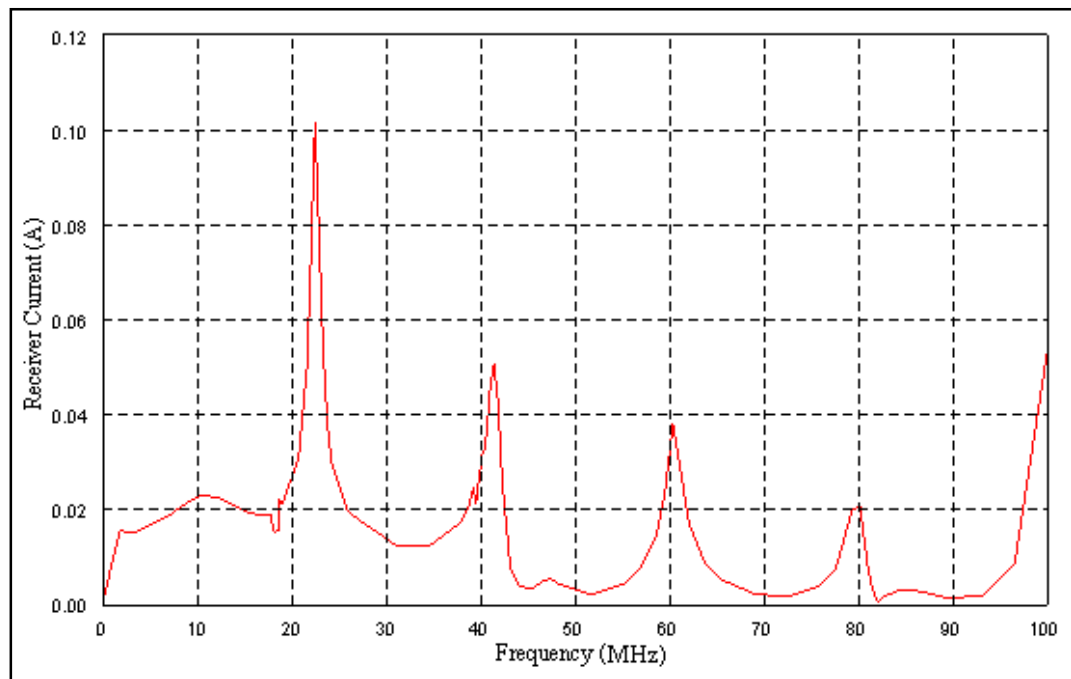
Figure 4.13. Wideband current response of transmitter coil with fo = 10 MHz (Array System)
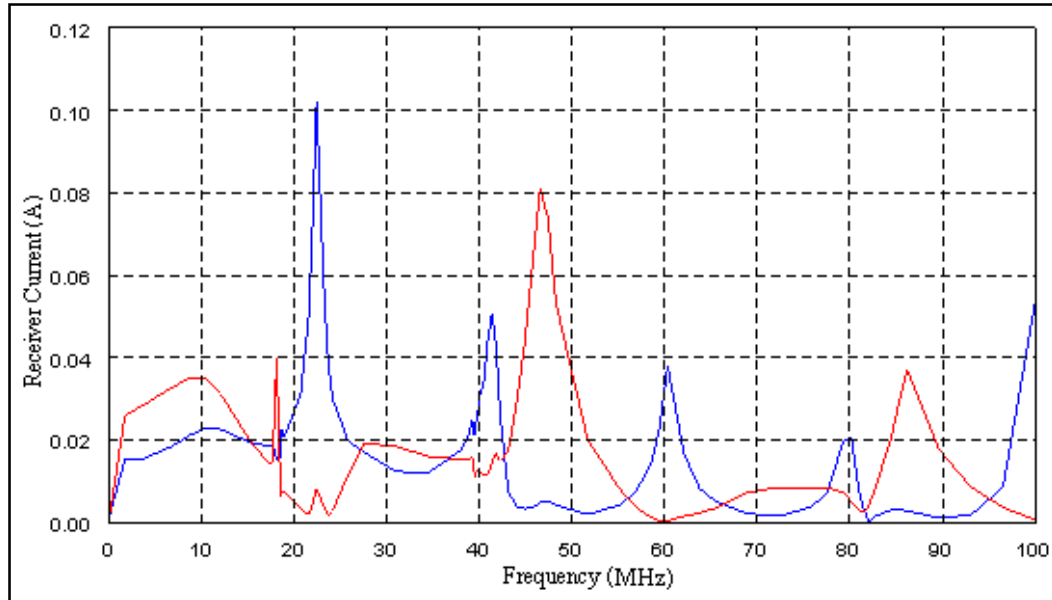
Figure 4.14. Wideband current response of transmitter coil with fo = 5 MHz and fo = 10 MHz (Array System)

4.4. MAXIMIZING FIELD INTENSITY

If we do not limit ourselves to use a limited space, we can use combinations as in Figure 4.15 in order to increase transmitter number.
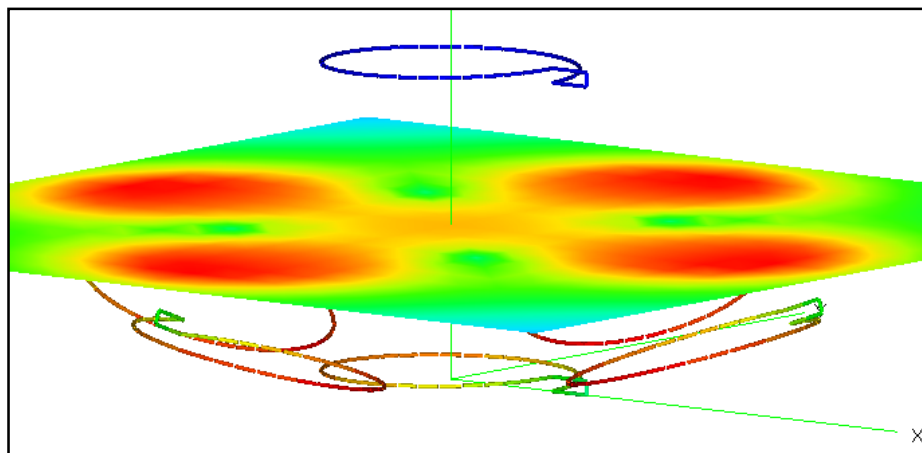
Figure 4.15. Array transmitter and single receiver system

In figure 4.16, we present current spectrum on the receiver side,
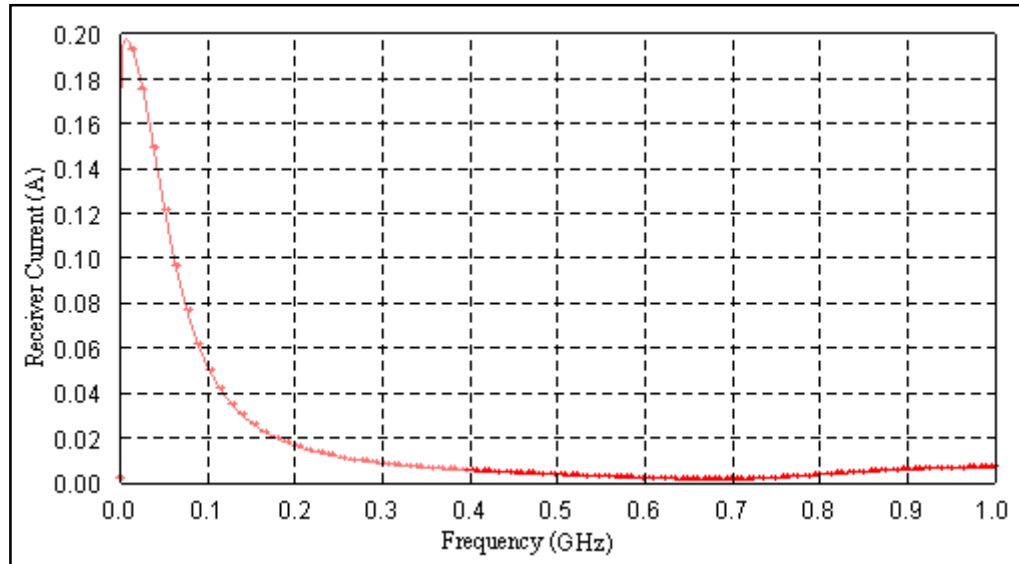
Figure 4.16. Received current spectrum for array transmitter and single receiver system

In figure 4.17, we increase radius of the receiver and observe extra reception on its self-resonant frequency.
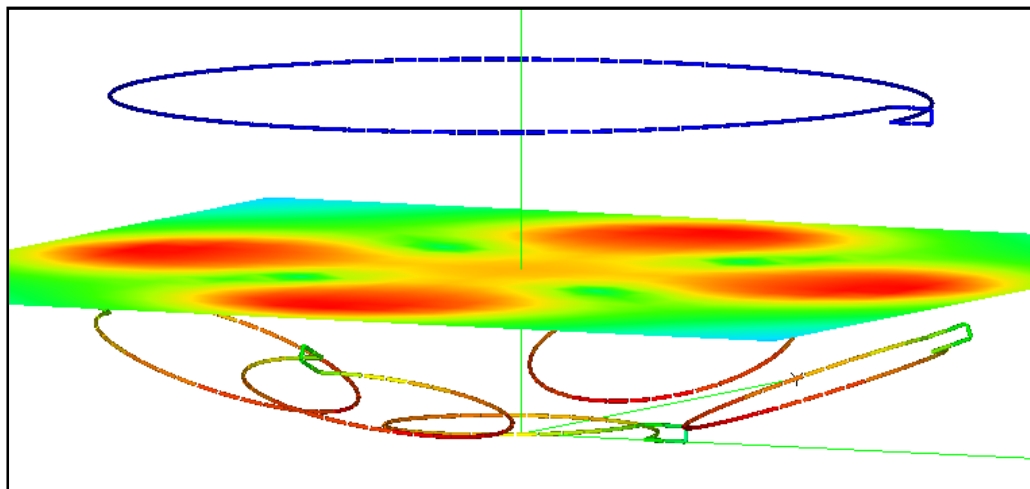
Figure 4.17. Array transmitter and single tuned receiver system
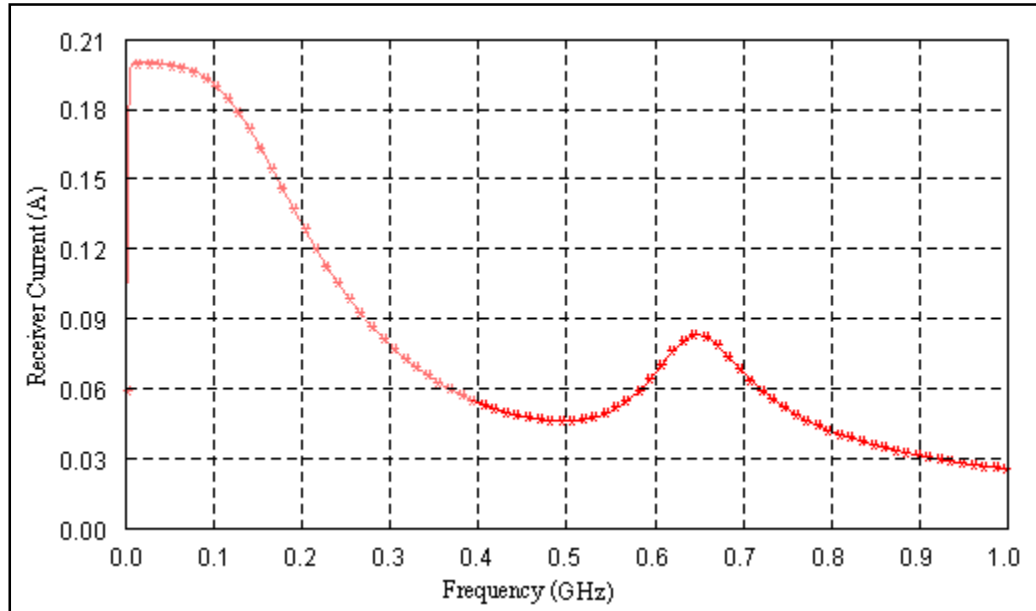
Figure 4.18. Received current spectrum for array transmitter and single tuned receiver system

4.5. CONCLUSION

Our studies on high Q RF resonators for strongly coupled resonant power transmission method clearly shown that power can be transferred further distances than loosely coupled coils. Wideband excitation of coils results in emission of waves in natural resonant frequencies of the coil – oscillator system. Upper harmonic emissions are also present in a narrow band high Q helix radiator. Strongly coupled inductive power transmission has small bandwidth utilization. This can be thought as downside of this system, but this problem can be solved by utilizing array transmitter and receiver systems with different resonant frequencies.

Even though phased array systems are common increasing transmitted and received power in the far field, but it is quite hard to pump and extract high power densities in the far field. Unlike the far-field where EM waves are usually characterized by a single polarization type (horizontal, vertical, circular, or elliptical), all four polarization types can be present in the near-field. The near-field is further divided into the "reactive" near-field and the "radiative" near-field. [28]

The reactive powers, which are present in very near field and circulate stored energy around it, cancel at resonance [28]. Using long-lived oscillatory resonant electromagnetic modes, with localized slowly-evanescent field patterns, efficient wireless non-radiative mid-range energy transfer can be realized. Non-radiative resonant coupling mechanism allows wireless power transmission with very low electromagnetic radiation.

Downside of strongly coupled resonant coils with high Q is small bandwidth utilization for power transmission. We propose to utilize coupled array of transmitters and receivers with different resonant frequencies in order to utilize different parts of the spectrum. Our coupled pairs clearly shows strong coupling to its resonant counterpart (receiver). FEKO simulations clearly show very small interaction between high Q transmitters. Most of the radiated energy is being captured by its resonant receiver pair.

Future studies can be focused on utilizing wider bandwidth with having multi resonant frequencies on the transmitter system. One approach may be synthesis of multiple resonant networks [16-18]; another may be upper harmonic maximization. Upper harmonic suppression is a common method in power electronics, but for wireless power transmission, it may be advantageous to utilize harmonics.

Different core, coil and surface materials and left handed dispersive mediums can be investigated to increase system performance.

Effective utilization of high power negative resistance oscillators may open a new perspective. Theoretical and practical nature of parametric resonance [27, 28] and damped oscillations can be studied. Near field dynamics of damped wideband coherent slow waves (1 Hz…1 MHz) can be studied [29-44].

Lastly, phase, speed, coherence related array transmitter combinations and wideband inductive receivers with high gain resemble exciting scientific research area to be explored.

APPENDIX A: BACKGROUND

A.1. MAXWELL'S FIELD EQUATIONS

In a region where μ and ε are continuous and in which there may be an electric charge density together with electric convection or conduction currents, we shall assume that the electric and magnetic quantities are connected by the equations;

$$\vec{\nabla} \cdot \vec{D}(r,t) = \rho(r,t) \tag{A.1}$$

$$\vec{\nabla} \cdot \vec{B}(r,t) = 0 \tag{A.2}$$

$$\vec{\nabla} \times \vec{E}(r,t) = -\frac{\partial \vec{B}(r,t)}{\partial t} \tag{A.3}$$

$$\vec{\nabla} \times \vec{H}(r,t) = \vec{\nabla} \times \frac{\vec{B}(r,t)}{\mu} = \frac{\partial \vec{D}(r,t)}{\partial t} + \vec{J}(r,t) \tag{A.4}$$

Where E(r, t) in V/m is the vector representing the electric field intensity, $\vec{D}(r,t)$ in C/m^2 is the electric flux density, $\vec{H}(r,t)$ in A/m is the magnetic field intensity, $\vec{B}(r,t)$ in T is the magnetic flux density, ρ(r, t) in C/m^3 is the charge density and $\vec{J}(r,t)$ in A/m^2 is the current density. All of the above electromagnetic field variables depend on the spatial position with respect to some coordinate system, r, and the elapsed time, t in s.

The electric and magnetic field vectors can be related through the constitutive relations,

$$\vec{D}(r,t) = \varepsilon_0 \varepsilon_r \vec{E}(r,t) \tag{A.5}$$

$$\vec{B}(r,t) = \mu_0 \mu_r \vec{H}(r,t) \tag{A.6}$$

$$\vec{J}(r,t) = \sigma \vec{E}(r,t) \tag{A.7}$$

Where, $\varepsilon_0 \approx 8.85 \times 10^{-12}$ F/m is the free space permittivity, ε_r is the material-dependent relative permittivity (also called the dielectric constant), and $\varepsilon = \varepsilon_0 \varepsilon_r$ simply permittivity; $\mu_0 \approx 1.257 \times 10^{-6}$ H/m is the free space permeability, μ_r is the material-dependent relative permeability, and $\mu = \mu_0 \mu_r$ simply permeability; and σ is the material-dependent conductivity expressed in S/m.

A.1.1. Physical Interpretation of Maxwell's Field Equations

The div operation characterizes how much a vector field linearly diverges and the curl operation characterizes the strength of the curl (rotation) in the field. Both relate to spatial operations, i.e. they do not involve any operations with respect to time.

$\vec{\nabla} \cdot \vec{D}(r,t) = \rho(r,t)$ means that static or dynamic charges in a given volume are responsible for a diverging electric field. That implies that there must be a distinct source and sink for the electric field since a field cannot possibly (linearly) diverge and start and end in the same location.

$\vec{\nabla} \cdot \vec{B}(r,t) = 0$ means that there is no physical medium which makes a magnetic field diverge. This equation comes from the observation that there are no magnetic charges known to physics. Note that magnetic charges are sometimes introduced in theoretical electrodynamics so as to simplify and beautify the derivation of certain theories.

$\vec{\nabla} \times \vec{E}(r,t) = -\partial \vec{B}(r,t)/\partial t$ means that a spatially varying (curling) electric field will cause a time-varying magnetic field. Alternatively, it can be rewritten as

$-\partial \vec{B}(r,t)/\partial t = \vec{\nabla} \times \vec{E}(r,t)$, i.e. a time-varying electric field will cause a curl in the magnetic field.

$\vec{\nabla} \times \vec{H}(r,t) = \partial \vec{D}(r,t)/\partial t + \vec{J}(r,t)$ can be read as follows. A spatially varying (curling) magnetic field will cause a time-varying electric field and, if existent, also a current through a medium capable of carrying a flow of electric charges. The equation can also be read as either a current flow through a medium or as a time-varying electric field producing a spatially curling magnetic field.

The first two equations yield separately an insight into the properties of the electric and magnetic field, respectively. The remaining two equations, however, show that both fields are closely coupled through spatial (curl) and temporal ($\partial/\partial t$) operations. We can also observe that the equations are entirely symmetric apart from the current density $\vec{J}(r,t)$. It turns out that this asymmetry is responsible for any radiation process occurring in nature, including the transmission and reception of electromagnetic waves.

Let's plug constitutive equations to Maxwell's equations and rewrite,

$$\vec{\nabla} \times \vec{E}(r,t) = -\mu_0 \mu_r \frac{\partial \vec{H}(r,t)}{\partial t} \qquad (A.8)$$

$$\vec{\nabla} \times \vec{H}(r,t) = \varepsilon_0 \varepsilon_r \frac{\vec{E}(r,t)}{\partial t} + \vec{J}(r,t) \qquad (A.9)$$

Let us assume first that there is a static current density $\vec{J}(r)$ available which, according to Equation (A.9), causes a spatially curling magnetic field $\vec{H}(r)$; however, it fails to generate a temporally varying magnetic field which means that $\partial \vec{H}(r)/\partial t = 0$. According to Equation (A.8), this in turn fails to generate a spatially and temporally varying electric field $\vec{E}(r)$. Therefore, a magnetic field is only generated in the location where we have a current density

$\vec{J}(r)$ present. Since we are interested in making a wave propagating in a wireless environment where no charges (and hence current densities) can be supported, a static current density $\vec{J}(r)$ is of little use.

Our observations, however, change when we start generating a time-varying current density $\vec{J}(r,t)$ which, according to Equation (A.9), generates a spatially and temporally varying magnetic field $\vec{H}(r,t)$. Clearly, $\partial \vec{H}(r,t)/\partial t \neq 0$ which, according to (A.9), generates a spatially and temporally varying electric field E(r, t), i.e. $\partial \vec{E}(r,t)/\partial t \neq 0$. With reference to (A.9), this generates a spatially and temporally varying magnetic field H(r, t), even in the absence of a current density $\vec{J}(r,t)$.

A wave is hence generated where the electric field stimulates the magnetic field and vice versa. This wave is electromagnetic (EM) wave, since it contains both magnetic and electric fields. From the above it is clear that such a wave can now propagate in space without the need of a charge-bearing medium; however, such a medium can certainly enhance or weaken the strength of the electromagnetic wave by means of an actively or passively created current density $\vec{J}(r,t)$.

From Maxwell's equations electric and magnetic components in explicit from can be derived by the help of two auxiliary concepts, the magnetic vector potential $\vec{A}(r,t)$ defined such that

$$\vec{\nabla} \times \vec{A}(r,t) = \vec{B}(r,t) \tag{A.10}$$

And the electric scalar potential $\Phi(r,t)$ defined such that

$$-\vec{\nabla} \cdot \Phi(r,t) = \vec{E}(r,t) + \frac{\partial \vec{A}(r,t)}{\partial t} \tag{A.11}$$

When plugged into Maxwell's equation, the two potentials manage to decouple, Equations (A.3) and (A.4), given that the following normalization is maintained between both auxiliary potentials;

$$\vec{\nabla} \cdot \vec{A}(r,t) + \mu\varepsilon \frac{\partial \Phi(r,t)}{\partial t} \equiv 0 \tag{A.12}$$

This normalization condition is also often referred to as the Lorentz gauge. When applied, it leads to a set of decoupled differential equations,

$$\nabla^2 \vec{A}(r,t) - \frac{1}{c^2}\mu\varepsilon \frac{\partial^2 \vec{A}(r,t)}{\partial t^2} = -\mu \cdot \vec{J}(r,t) \tag{A.13}$$

$$\nabla^2 \Phi(r,t) - \frac{1}{c^2}\mu\varepsilon \frac{\partial^2 \Phi(r,t)}{\partial t^2} = -\varepsilon^{-1} \cdot \rho(r,t) \tag{A.14}$$

Where, $c = 1/\sqrt{\varepsilon\mu}$ is the speed of light in the material under consideration, and ∇^2 is the Laplace operator, the exact mathematical description of which depends on the coordinate system of choice.

The two equations (A.13) and (A.14) are often referred to as the wave equations, and solved in a fairly standard manner in dependency of prevailing sources and boundary conditions for $\vec{J}(r,t)$ and ρ(r, t), to arrive at

$$\vec{A}(r,t) = \frac{\mu}{4\pi} \oint_{V'} \frac{\vec{J}(r',t - \frac{|r-r'|}{c})}{|r-r'|} dV' \tag{A.15}$$

$$\Phi(r,t) = \frac{1}{4\pi\varepsilon} \oint_{V'} \frac{\rho(r',t - \frac{|r-r'|}{c})}{|r-r'|} dV' \tag{A.16}$$

Which are often referred to as **retarded potentials**. The reason for this nomenclature is that the effects of current density and charge time t and position r' are felt at position r after a time delay of $|r - r'|/c$, which is exactly the time the electromagnetic wave needs to propagate.

A.1.2. Propagation Equation, Electrodynamic Potentials and Hertz Vector

Taking the curl of (A.4) gives when μ is constant,

$$\vec{\nabla} \times \left(\vec{\nabla} \times \vec{B}(r,t) \right) = \vec{\nabla} \left(\vec{\nabla} \cdot \vec{B}(r,t) \right) - \nabla^2 \cdot \vec{B}(r,t)$$
$$= \mu \left[\gamma \left(\vec{\nabla} \times \vec{E}(r,t) \right) + \varepsilon \frac{\partial}{\partial t} \left(\vec{\nabla} \times \vec{E}(r,t) \right) \right] \tag{A.17}$$

Substitution for $\vec{\nabla} \cdot \vec{B}(r,t)$ from (A.2) and for $\vec{\nabla} \times \vec{E}(r,t)$ from (A.3) give,

$$\nabla^2 \times \vec{E}(r,t) = \mu\gamma \frac{\partial \vec{E}(r,t)}{\partial t} + \mu\varepsilon \frac{\partial^2 \vec{E}(r,t)}{\partial t^2} \tag{A.18}$$

These are the propagation equations for the magnetic induction and the electric intensity. The first term on the right represents a dissipation of energy as heat or a damping term in the wave which is absent in insulating mediums where γ is zero. We have used extensively an electrostatic scalar potential whose negative gradient is the electric field and a magnetostatic vector potential whose curl is the magnetic induction and whose divergence is zero. We wish to extend these potential definitions to include rapidly fluctuating fields. Let us, therefore, choose a general magnetic vector potential $\vec{A}$ whose curl always gives the magnetic induction $\vec{B}$ and which, for steady fields, reduces to the magnetostatic vector potential. Thus,

$$\vec{B} = \vec{\nabla} \times \vec{A} \tag{A.18}$$

Eliminating $\vec{B}$ by (A.3) and changing the differentiation order give

$$\vec{\nabla} \times \vec{E} = -\vec{\nabla} \times \frac{\partial \vec{A}}{\partial t} \qquad (A.19)$$

Integration of this removes the curls but adds an integration constant whose curl is zero and hence must be the gradient of a scalar. Thus

$$\vec{E} = -\frac{\partial \vec{A}}{\partial t} - \nabla \Phi \qquad (A.20)$$

Φ is called the electric potential, which is identical with the electrostatic potential for static fields. It is convenient, but not necessary to have A and Φ satisfy the same propagation equations as $\vec{E}$ and $\vec{B}$,

$$\nabla^2 \vec{A} = \mu\gamma \frac{\partial \vec{A}}{\partial t} + \mu\varepsilon \frac{\partial^2 \vec{A}}{\partial t^2} \qquad (A.21)$$

$$\nabla^2 \Phi = \mu\gamma \frac{\partial \Phi}{\partial t} + \mu\varepsilon \frac{\partial^2 \Phi}{\partial t^2} \qquad (A.22)$$

This gives another relation between A and Φ for if we take the divergence of both sides of (A.20) then, if ρ is zero, $\nabla \cdot E$ is zero by (A.1) so that

$$\nabla^2 \Phi = -\frac{\partial \vec{\nabla} \cdot \vec{A}}{\partial t} \qquad (A.23)$$

Comparison of this with (A.22) shows that the latter will hold if

$$\vec{\nabla} \cdot \vec{A} = -\mu\gamma\Phi - \mu\varepsilon\frac{\partial\Phi}{\partial t} \tag{A.24}$$

To show that (A.21) and (A.24) are consistent, take the gradient of both sides of (A.24), expand the left side by using again the vector relation at the first of this article, and substitute for $\vec{\nabla} \times \vec{B}$ from (A.4). On the right side substitute for $\nabla\Phi$ from (A.20). Canceling terms appearing on both sides of the resultant equation gives (A.21). Electromagnetic field may be described by means of a single vector $\vec{Z}$, called the Hertz vector; $\vec{A}$ and Φ can be obtained by the equations

$$\vec{A} = \mu\gamma\vec{Z} + \mu\varepsilon\frac{\partial\vec{Z}}{\partial t}, \qquad \Phi = -\vec{\nabla} \cdot \vec{Z} \tag{A.25}$$

These equations satisfy (A.24) and also (A.20) if we take

$$\vec{E} = \vec{\nabla}\left(\vec{\nabla} \cdot \vec{Z}\right) - \nabla^2\vec{Z} = \vec{\nabla} \times \left(\vec{\nabla} \times \vec{Z}\right) \tag{A.26}$$

$$\nabla^2\vec{Z} = \mu\gamma\frac{\partial\vec{Z}}{\partial t} + \mu\varepsilon\frac{\partial^2\vec{Z}}{\partial^2 t} \tag{A.27}$$

The magnetic induction is given by (A.18) and (A.19) in terms of $\vec{Z}$.

$$\vec{B} = \mu\gamma\vec{\nabla} \times \vec{Z} + \mu\varepsilon\frac{\partial\vec{\nabla} \times \vec{Z}}{\partial t} \tag{A.28}$$

Equation (A.27) contains all the properties of the electromagnetic wave. In non-conducting mediums the elimination of Φ from (A.20) and (A.24) gives

$$\vec{E} = -\frac{\partial \vec{A}}{\partial t} + \frac{1}{\mu\varepsilon}\int \vec{\nabla}\vec{\nabla}\cdot \vec{A}dt = -\frac{\partial \vec{A}'}{\partial t} \qquad \vec{B} = \vec{\nabla}\times\vec{A}' \qquad\qquad \text{(A.29)}$$

When $\rho = 0$, the new vector potential $\vec{A}'$ has zero divergence.

A.1.3. Propagation in Dispersive Medium

A pulse or "signal" of any specified initial form may be constructed by superposition of harmonic wave trains of infinite length and duration. The velocities with which the constant-phase surfaces of these component waves are propagated have been shown to depend on the parameters ε, μ and σ. In particular, if the medium is non-conducting and the quantities ε and μ are independent of the frequency of the applied field, the phase velocity proves to be constant and the signal is propagated without distortion. The presence of conductivity, on the other hand, leads to a functional relation between the frequency and the phase velocity, as well as to attenuation. Consequently the harmonic components suffer relative displacements in phase in the direction of propagation and the signal arrives at a distant point in a modified and perhaps unrecognizable form. A medium in which the phase velocity is a function of the frequency is dispersive medium.

At sufficiently high frequencies a substance may exhibit dispersive properties even when the conductivity σ due to free charges is wholly negligible. In dielectric media the phase velocity is related to the index of refraction n by $v = c/n$, where $n = \sqrt{\kappa_e \kappa_m}$. At frequencies less than 100 MHz, the specific inductive capacities of most materials are substantially independent of the frequency, but they manifest a marked dependence on frequency within a range which often begins in the ultra- high-frequency radio region and extends into the infrared and beyond. Thus, while the refractive index of water at frequencies less than 100 MHz is about 9, it fluctuates at frequencies in the neighborhood of 10 GHz. and eventually drops to 1.32 in the infrared. Apart from solutions or crystals of ferromagnetic salts, the

dispersive action of a nonconductor can be attributed wholly to a dependence of κ_e on the frequency.

All modern theories of dispersion take into account the molecular constitution of matter and treat the molecules as dynamical systems possessing natural free periods which are excited by the incident field. Both the classical and the quantum theories of dispersion undertake to calculate the displacement of charge from the center of gravity of an atomic system as a function of the frequency and intensity of the disturbing field. After a process of averaging over the atoms contained within an appropriately chosen volume element, one obtains an expression for the polarization of the medium; that is to say, the dipole moment per unit volume. The classical result corresponds closely in form to the quantum mechanical formula and leads in most cases to an adequate representation of the index of refraction as a function of frequency. The electric polarization in the neighborhood of a resonance frequency can be expressed approximately by the real part of,

$$\vec{P} = \frac{a^2}{\overline{\omega}_0^2 - \omega^2 - i\omega g}\varepsilon_0 \vec{E} \qquad (A.30)$$

By the electric field intensity, we shall now understand the real part of the complex vector

$$\vec{E} = \vec{E}_0 e^{-\omega t} \qquad (A.31)$$

The constant a^2 is directly proportional to the number of oscillators per unit volume whose resonant frequency is ω_0. The constant $\overline{\omega}_0$ is related to this resonant frequency by

$$\overline{\omega}_0^2 = \omega_0^2 - \frac{1}{8}a^2 \qquad (A.32)$$

Such that $\overline{\omega}_0 \to \omega_0$ at sufficiently small densities of matter. The constant g takes account of dissipative, quasi-frictional forces introduced by collisions of the molecules. The constants

$\bar{\omega}_0$ and g which characterize the molecules of a specific medium must be determined from experimental data. At sufficiently low incident frequencies ω, the polarization P according to equation A.30 approaches a constant value

$$\vec{P} = \frac{a^2}{\bar{\omega}_0^2} \varepsilon_0 \vec{E} \tag{A.33}$$

And, since the specific inductive capacity is related to the polarization by;

$$\vec{P} = (\kappa - 1)\varepsilon_0 \vec{E} \tag{A.34}$$

κ can be expressed in terms of the molecular constants;

$$\kappa = 1 + \frac{a^2}{\bar{\omega}_0^2} \tag{A.35}$$

When, however, the incident frequency is increased, further neglect of the two remaining terms in the denominator becomes inadmissible. In that case we shall define by analogy a complex inductive capacity κ' through either of the equations,

$$\vec{P} = (\kappa' - 1)\varepsilon_0 \vec{E}, \qquad \vec{D} = \kappa' \varepsilon_0 \vec{E}, \tag{A.36}$$

Hence from (A.30) we obtain;

$$\kappa' = 1 + \frac{a^2}{\bar{\omega}_0^2 - \omega^2 - i\omega g} \tag{A.37}$$

In terms of this complex parameter the Maxwell equations in a medium whose magnetic permeability is μ_0 are,

$$\vec{\nabla} \times \vec{E} + \mu_0 \frac{\partial \vec{H}}{\partial t} = 0, \qquad \vec{\nabla} \times \vec{H} - \varepsilon_0 \kappa' \frac{\partial \vec{E}}{\partial t} = 0, \tag{A.38}$$

As a consequence of which the rectangular components of the field vectors satisfy the wave equation;

$$\nabla^2 \Phi - \varepsilon_0 \mu_0 \kappa' \frac{\partial^2 \Phi}{\partial t^2} = 0, \tag{A.39}$$

A plane wave solution of (A.39) is represented by,

$$\Phi = \Phi_0 e^{ikz - i\omega t}, \tag{A.40}$$

Where,

$$k = \frac{\omega}{c} \sqrt{\kappa'} = \alpha + i\beta, \tag{A.41}$$

So that,

$$\kappa' = \frac{c^2}{\omega^2} (\alpha + i\beta)^2. \tag{A.42}$$

The wave is propagated with a velocity $v = \omega / \alpha = c / n$, but α and the refractive index are now explicit functions of the frequency obtained by introducing (A.37) into (A.42). In gases and vapors the density of polarized molecules is so low that κ' differs by a very small amount from unity. The constant a^2 is therefore small, so that $\bar{\omega}_0$ differs by a negligible amount from the natural frequency ω_0 and the root of κ' can be obtained by retaining the first two terms of a binomial expansion. Thus,

$$\frac{c}{\omega}(\alpha + i\beta) = 1 + \frac{1}{2}\frac{a^2}{\omega_0^2 - \omega^2 - i\omega g} \qquad (A.43)$$

When the impressed frequency ω is sufficiently low, the last two terms of the denominator may be neglected so that,

$$\frac{\alpha c}{\omega} = n = 1 + \frac{a^2}{2\omega_0^2} \qquad (A.44)$$

The index of refraction and consequently the phase velocity in this case are independent of the frequency; there is no dispersion. If the impressed frequency ω is appreciable with respect to the resonant frequency ω_0 but does not approach it too closely, the damping term may still be neglected. $\left|\omega_0^2 - \omega^2\right| \gg \omega g$,

$$\frac{\alpha c}{\omega} = n = 1 + \frac{1}{2}\frac{a^2}{\omega_0^2 - \omega^2} \qquad (A.45)$$

The attenuation factor is zero and the medium is transparent, but the refractive index and the phase velocity are functions of the frequency.

If $\omega < \omega_0$, n will be greater than unity and an increase in ω leads to an increase in n and a decrease in v.

If $\omega > \omega_0$, the refractive index is less than unity but an increase in ω still results in an increase in the numerical value of n. The dispersion in this case is said to be normal.

If ω approach the resonance frequency ω_0, with resolving (A.43) into its real and imaginary parts,

$$n = \frac{\alpha c}{\omega} = 1 + \frac{a^2}{2} \frac{\omega_0^2 - \omega^2}{\left(\omega_0^2 - \omega^2\right)^2 + \omega^2 g^2}$$

<div align="right">(A.46)</div>

$$\beta = \frac{a^2}{2c} \frac{g}{\left(\omega_0^2 - \omega^2\right)^2 + \omega^2 g^2}$$

A molecule is a complicated dynamical system possessing infinite series of natural frequencies, each affecting the reaction of the molecule to the incident field. The location of these natural periods cannot be determined by classical theory; by proper adjustment of constants to experimental data, an empirical dispersion formula can be set up, of which (A.37) is a typical term and which is found to satisfy the observed data over an extensive range of frequencies.

A.2. MAGNETOSTATIC VECTOR POTENTIAL AND MAGNETIC FLUX DENSITY OF CIRCULAR LOOP

Wire segment and loops with stationary electric currents (electric charges moving with constant speeds) creates static magnetic flux densities around the wire. Ampère's experiments on the interaction between two small loops of electric current have shown that they also interact via a mechanical force, much the same way that electric charges interact. Magnetic flux density B is defined as,

$$dB = \frac{\mu_0 I}{4\pi} \frac{\vec{dl} \times \overrightarrow{a_{qp}}}{\left|r_p - r_q\right|^2}$$

<div align="right">(A.47)</div>

Which expresses the small element dB of the static magnetic field set up at the field point $P(r_p, \varphi_p, z_p)$ by a small line element dl of stationary current I at the source point $\vec{r}_q$. The SI unit for the magnetic field, sometimes called the magnetic flux density or magnetic induction, is Tesla (T).
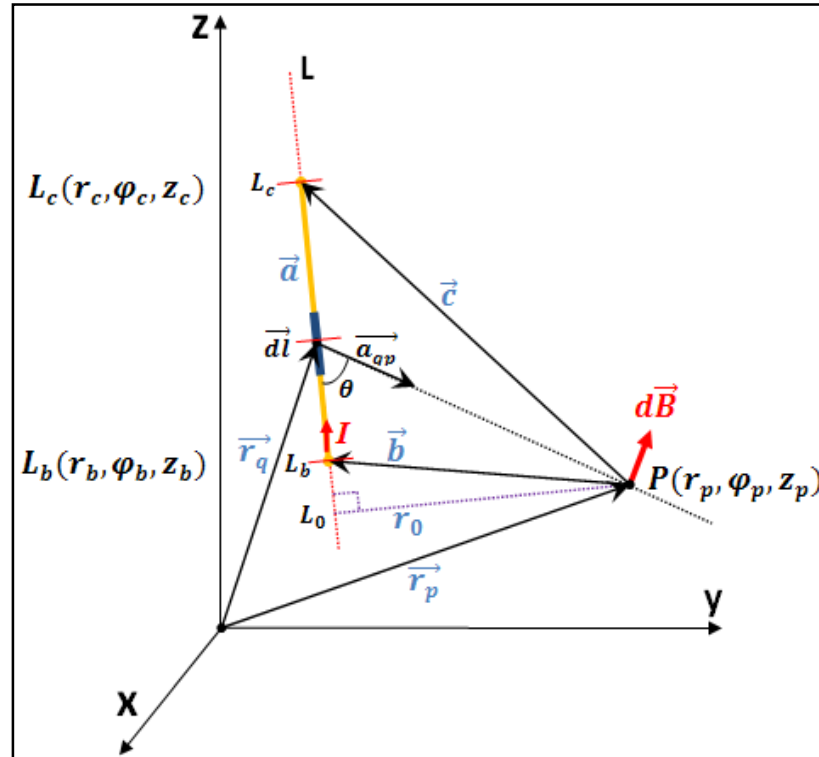
Figure A.1. Thin wire arbitrarily placed in space (L_b to L_c) and observer point P

The Biot-Savart superposition integral can be derived analytically for relatively few configurations. Nevertheless, its evaluation amounts to no more than a summation of the field contributions from each of the current elements. Many practical current distributions can be approximated by, connected straight-line current segments, or current "sticks."

The Biot-Savart law is used to find the field at an arbitrary observer position $\vec{r}_p$ associated with a current stick having an arbitrary location. The current stick, shown in Figure A.1 is represented by a vector $\vec{a}$. Thus, the current is uniformly distributed between the base of this vector at $\vec{r}_p + \vec{b}$ and the tip of the vector at $\vec{r}_p + \vec{c}$. The source coordinate $\vec{r}_q$ is located along the current stick. Integration over the length of the current stick is carried out to obtain an expression for B. Because the current stick does not represent a solenoidal current density at its ends, the field derived is of physical significance only if used in conjunction with other current sticks that together represent a continuous current distribution. In Figure A.1 L is the

source coordinate denotes the position along the stick. The origin of this coordinate is at the point on a line through the stick that is closest to the observer coordinate.

The cross product solution;

$$\vec{dl} \times \overrightarrow{a_{qp}} = \left|\vec{dl}\right|\left|\overrightarrow{a_{qp}}\right|\sin\theta \tag{A.48}$$

where dl is the differential along the line current and

$$\left|r_p - r_q\right| = (l^2 + r_0^2)^{\frac{1}{2}} \tag{A.49}$$

Integration of the Biot-Savart law is first performed over the cross-section of the stick. The cross-sectional dimensions are small, so during this integration, the integrand remains essentially constant. Thus, the current density is replaced by the total current and the integral reduced to one on the axial coordinate L of the stick.

$$\vec{B}(r,\varphi,z) = \frac{\mu_0 I}{4\pi}\int_{L_b}^{L_c} \frac{\vec{dl} \times \overrightarrow{a_{qp}}}{\left|r_p - r_q\right|^2} \tag{A.50}$$

This integral is expressed in terms of the source coordinate integration variable L as

$$\vec{B}(r,\varphi,z) = \frac{\mu_0 I}{4\pi}\int_{L_b}^{L_c} \frac{(\vec{c} \times \vec{a})\vec{dl}}{\left|\vec{a}\right|(L^2 + r_0^2)^{\frac{3}{2}}} \tag{A.51}$$

This integral is carried out to obtain;

$$\vec{B}(r,\varphi,z) = \frac{\mu_0 I}{4\pi} \frac{(\vec{c} \times \vec{a})}{|\vec{a}|} \left[\frac{L}{r_0^2 (L^2 + r_0^2)^{\frac{1}{2}}} \right]_{L_b}^{L_c} \tag{A.52}$$

Applying limits;

$$\vec{B}(r,\varphi,z) = \frac{\mu_0 I}{4\pi} \frac{(\vec{c} \times \vec{a})}{|\vec{a}|} \left[\frac{L_c}{r_0^2 (L_c^2 + r_0^2)^{\frac{1}{2}}} - \frac{L_b}{r_0^2 (L_b^2 + r_0^2)^{\frac{1}{2}}} \right] \tag{A.53}$$

Plugging L_b and L_c into (A.53),

$$\vec{B}(r,\varphi,z) = \frac{\mu_0 I}{4\pi} \frac{(\vec{c} \times \vec{a})}{|\vec{a}|} \left[\frac{\frac{\vec{a} \cdot \vec{c}}{|\vec{a}|}}{r_0^2 |\vec{c}|} - \frac{\frac{\vec{a} \cdot \vec{b}}{|\vec{a}|}}{r_0^2 |\vec{b}|} \right] \tag{A.54}$$

So that becomes an expression for the field intensity at the observer location expressed in terms of vectors a, b, and c that serve to define the relative location of the current stick.

$$\vec{B}(r,\varphi,z) = \frac{\mu_0 I}{4\pi} \frac{(\vec{c} \times \vec{a})}{|\vec{c} \times \vec{a}|^2} \left[\frac{\vec{a} \cdot \vec{c}}{|\vec{c}|} - \frac{\vec{a} \cdot \vec{b}}{|\vec{b}|} \right] \tag{A.55}$$

Magnetic flux density field vector diagram for a segment wire placed along r axis starting from $L_b(r,\varphi,z) = (-10,180,0)$ and finish at $L_c(r,\varphi,z) = (10,180,0)$ is presented in Figure A.1. (r-z plane cross section of the wire $\varphi_p = 90°$),

A.2.1. Magnetostatic Field of Polygon Thin Wire Loop
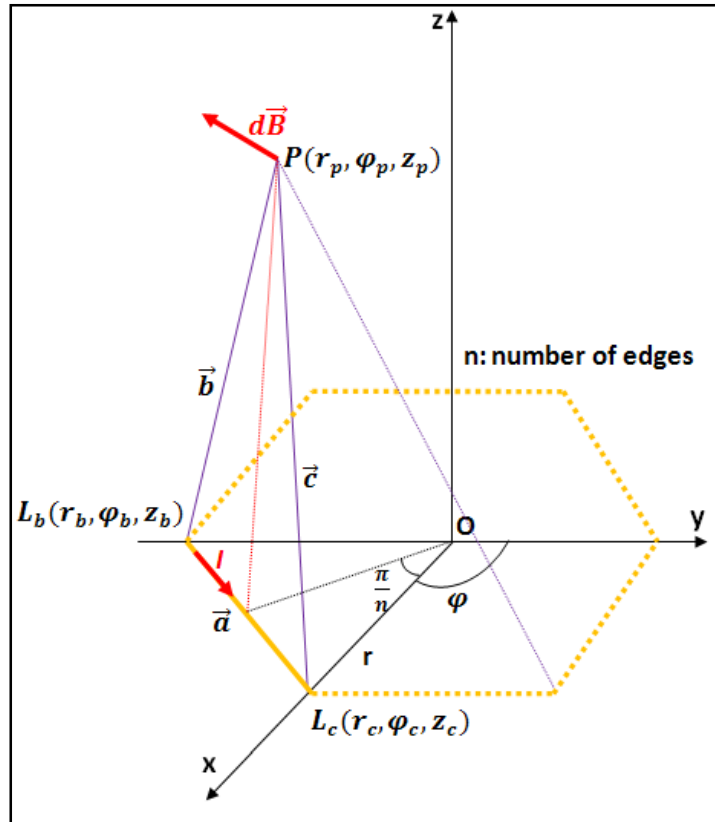
Figure A.2. Superposition of B field from a polygon-wire loop

Polygon wire loop can be constructed from minimum of three wire segments. Increasing the number of corners or polygons result in better estimation of B field at any arbitrary position $P(r, \varphi, z)$. A generic formulation is derived to numerically calculate superposition of $\vec{B}_r, \vec{B}_\varphi$ and $\vec{B}_z$ vectors for each segment of the polygon at point $P(r, \varphi, z)$.

For each polygon segment, starting $L_b(r, \varphi, z)$ and finishing $L_c(r, \varphi, z)$ points calculated and superposition accumulation of $\vec{B}_r, \vec{B}_\varphi$ and $\vec{B}_z$ vectors at any arbitrary point $P(r, \varphi, z)$ is calculated. From $\vec{B}_r, \vec{B}_\varphi$ and $\vec{B}_z$ vectors $\vec{B}_{total}$ is derived.

$$\vec{B}_{total}(r,\varphi,z) = \sqrt{\vec{B}_r(r,\varphi,z)^2 + \vec{B}_\varphi(r,\varphi,z)^2 + \vec{B}_z(r,\varphi,z)^2} \qquad (A.56)$$

If we locate loop co-axial with z axis; along the z-axis $\vec{B}_r$ and $\vec{B}_\varphi$ components cancel out due to symmetry. Magnitude of magnetic flux density vectors along the z-axis is shown in Figure A.3.

Figure A.3. $\vec{B}_r$, $\vec{B}_\varphi$, $\vec{B}_z$ and $\vec{B}_t$ values along the z axis (I = 100 A, r = 4 m, Pn=60)

Similarly r-axis scan of magnetic flux density magnitudes for a loop co-axial with z-axis is presented in Figure A.4,
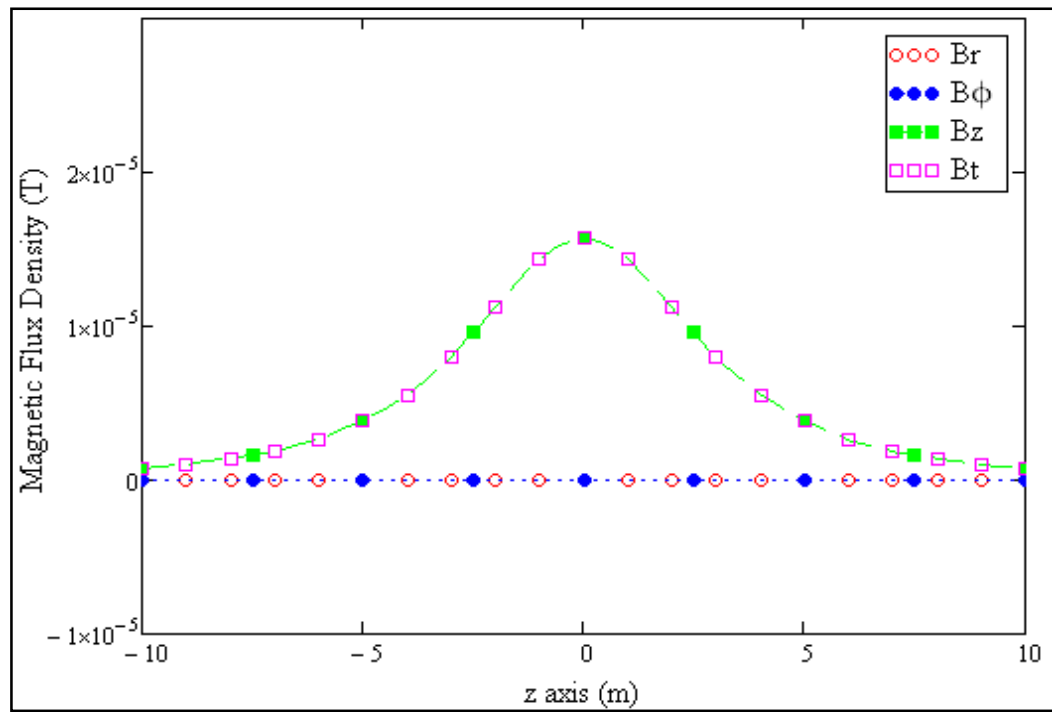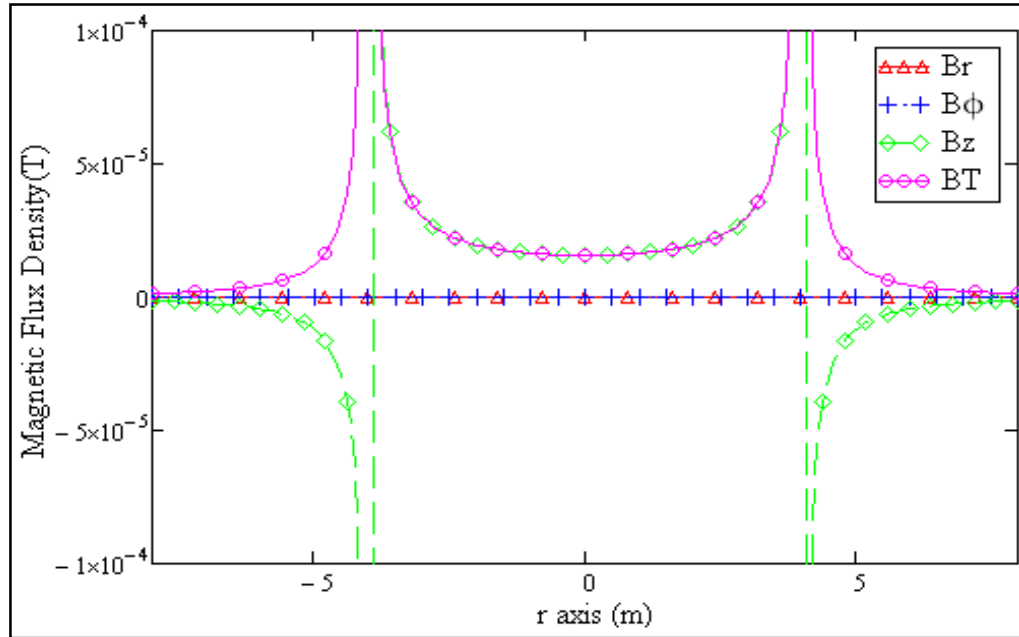
Figure A.4. $\vec{B}_r$, $\vec{B}_\varphi$, $\vec{B}_z$ and $\vec{B}_t$ values along the r axis (I = 100 A, r = 4 m, Pn=60)

Applied DC current applied on loop wire directly proportional to the magnetic flux density, Figure A.5 represents r-axis $\vec{B}_t$ magnitude graph 10 cm. above the r-axis, z_p = 10 cm.
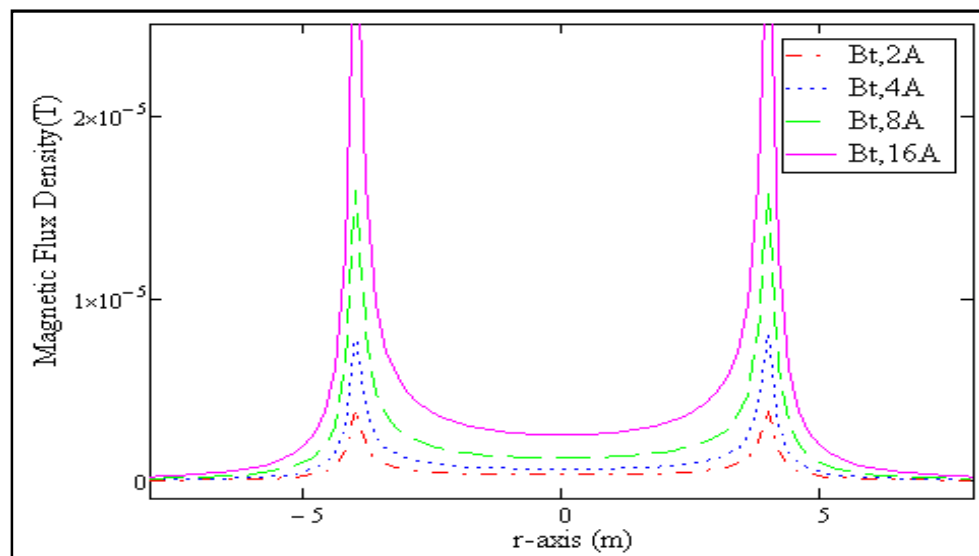
Figure A.5. $\vec{B}_t$ along r axis with increasing I current

Magnetic flux density of a polygon loop with constant current will establish static field distribution that does not change with time (Figure A.6).

Different configurations of polygon loop placements will result in different magnetic flux density field vector distribution around the polygon loop. Magnetic fields between two co-axially placed polygon loops vanish as two loops pushed each other.

Figure A.6. Cross section of magnetic flux density vector field with three inner placed loops

APPENDIX B : TABLES

B.1. DC Resistance of Stranded Copper at 20 Celsius Degrees

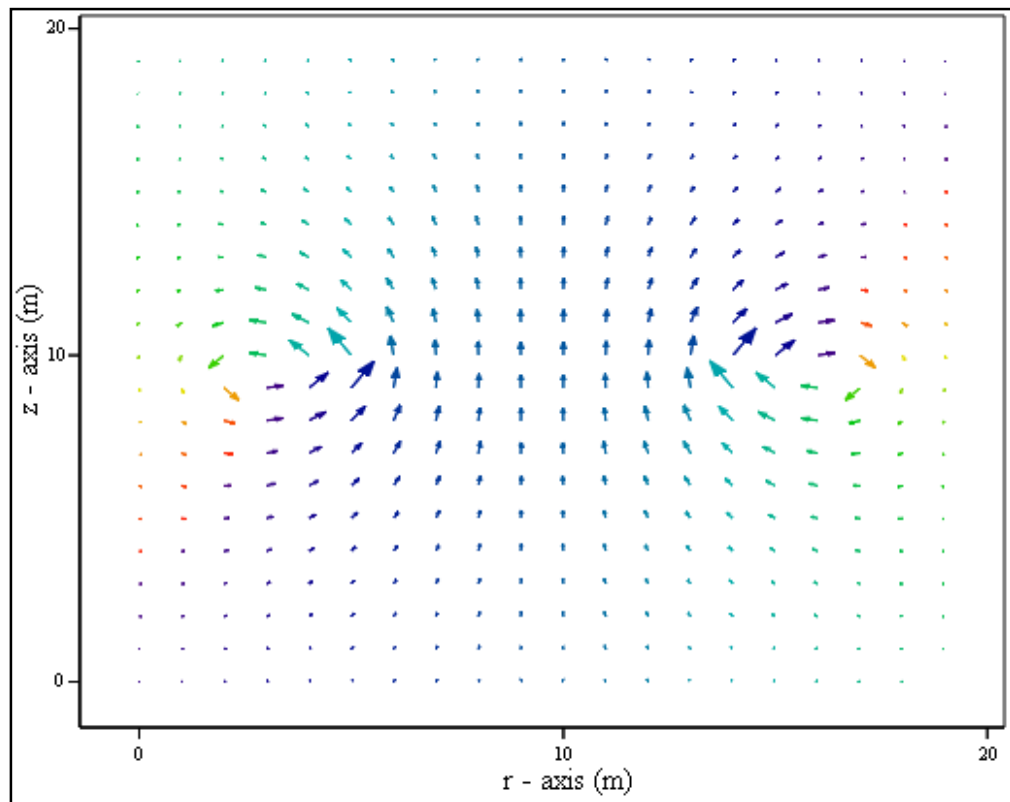| AWG	Diameter	DCR @ 20 Bare Copper	AWG	Diameter	DCR @ 20 Bare Copper
32	0.236 mm	543.6 ohms/Km	18	1.154 mm	20.0 ohms/Km
30	0.297 mm	321.5 ohms/Km	18	1.143 mm	21.9 ohms/Km
30	0.305 mm	311.4 ohms/Km	18	1.219 mm	18.7 ohms/Km
29	0.343 mm	251.3 ohms/Km	18	1.118 mm	21.9 ohms/Km
28	0.373 mm	204.1 ohms/Km	18	1.118 mm	22.3 ohms/Km
28	0.373 mm	202.4 ohms/Km	18	1.346 mm	22.9 ohms/Km
27	0.432 mm	164.4 ohms/Km	16	1.524 mm	12.5 ohms/Km
26	0.483 mm	127.3 ohms/Km	16	1.488 mm	13.8 ohms/Km
26	0.483 mm	142.1 ohms/Km	16	1.372 mm	14.4 ohms/Km
26	0.483 mm	118.1 ohms/Km	16	1.422 mm	13.8 ohms/Km
26	0.457 mm	145.7 ohms/Km	16	1.448 mm	13.8 ohms/Km
25	0.533 mm	100.7 ohms/Km	16	1.448 mm	14.1 ohms/Km
24	0.610 mm	78.7 ohms/Km	16	1.448 mm	13.8 ohms/Km
24	0.559 mm	88.9 ohms/Km	14	1.842 mm	8.86 ohms/Km
24	0.559 mm	88.9 ohms/Km	14	1.930 mm	8.53 ohms/Km
24	0.610 mm	76.1 ohms/Km	14	1.715 mm	8.53 ohms/Km
24	0.559 mm	92.5 ohms/Km	14	1.803 mm	8.86 ohms/Km
22	0.762 mm	50.5 ohms/Km	14	1.778 mm	8.86 ohms/Km
22	0.711 mm	56.1 ohms/Km	12	2.337 mm	5.58 ohms/Km
22	0.762 mm	46.9 ohms/Km	12	2.159 mm	5.91 ohms/Km
22	0.737 mm	55.1 ohms/Km	12	2.235 mm	5.58 ohms/Km
22	0.737 mm	52.8 ohms/Km	12	2.261 mm	5.58 ohms/Km
22	0.711 mm	59.4 ohms/Km	12	2.540 mm	5.58 ohms/Km
21	0.876 mm	37.1 ohms/Km	10	2.845 mm	3.61 ohms/Km
20	0.965 mm	31.5 ohms/Km	10	2.743 mm	3.94 ohms/Km
20	0.914 mm	35.8 ohms/Km	10	2.921 mm	3.28 ohms/Km
20	0.965 mm	29.1 ohms/Km	8	3.505 mm	2.17 ohms/Km
20	0.914 mm	34.4 ohms/Km	8	4.064 mm	2.13 ohms/Km
20	0.914 mm	35.4 ohms/Km	8	4.115 mm	2.13 ohms/Km
20	0.914 mm	34.1 ohms/Km	6	5.055 mm	1.35 ohms/Km
20	1.02 mm	36.4 ohms/Km	4	6.350 mm	1.28 ohms/Km
19	1.07 mm	22.9 ohms/Km	4	6.400 mm	0.85 ohms/Km

REFERENCES

1. C. Canbay, *Antennas and Propagation I*, II, Department of Electrical and Electronics Engineering, Yeditepe University, 2007.

2. *Wireless energy transfer,* http://en.wikipedia.org/wiki/Wireless_energy_transfer

3. *Resonant energy transfer,* http://en.wikipedia.org/wiki/Resonant_inductive_coupling

4. A. Haus, A. Hermann, and J. R. Melcher, *Electromagnetic Fields and Energy*. (MIT OpenCourseWare). http://ocw.mit.edu, 2009.

5. A. Haus, A. Hermann, and J. R. Melcher, *Solutions Manual for Electromagnetic Fields and Energy*. (MIT OpenCourseWare). http://ocw.mit.edu, 2009.

6. M. Zahn, Electromagnetic *Field Theory: A Problem Solving Approach*. (MIT OpenCourseWare). http://ocw.mit.edu, 2009.

7. A. Kurs, A. Karalis, R. Moffatt, J. D. Joannopoulos, P. Fisher, M. Soljacic, "Wireless Power Transfer via Strongly Coupled Magnetic Resonances", *Massachusetts Institute of Technology, 2007 Science*, Vol. 317. no. 5834, pp. 83 – 86, 2007.

8. K. E. Oughstun, "Pulse Propagation in a Linear, Causally Dispersive Medium", *Proceedings of the IEEE*, Vol 79, No. 10, 1991.

9. K. E. Oughstun and N. A. Cartwright, "Physical Significance of the Group Velocity in Dispersive", *Ultrashort Guassian Pulse Dynamics, Journal of Modern Optics*, Vol. 52, No. 8, pp. 1089-1104, 2005.

10. K. E. Oughstun, P. Wyns, and D. Foty, "Numerical Determination of the Signal Velocity in Dispersive Pulse Propagation", *Optical Society of America*, Vol. 6, No. 9, pg. 1430, 1989.

11. U. Miyagawa, *B field Calculation at CERN Atlas Project*, www.hep.man.ac.uk, 2008.

12. G. Johnson, *Solid State Tesla Coil*, Ch. 6 Resistance of Coil, Princeton University, 2001.

13. F.E. Terman, *Electronic and Radio Engineering*, 4th edition 1955.

14. R.G. Medhurst, "Single-Layer Solenoids", *Wireless Engineer*, February 1947.

15. G. Grandi, M.K. Kazimierczuk, A. Massarini, "Optimal Design of Single-Layer Solenoid Air-Core Inductors for High Frequency Applications", *Circuit Systems*, Vol. 1, pg. 358-361, 1997.

16. A.C.M de Queiroz, "Synthesis of Multiple Resonance Networks", *EE/COPPE,* Universidade Federal do Rio de Janerio, Brazil.

17. A.C.M de Queiroz, "The Triple Resonance Network With Sinusoidal Excitation", *EE/COPPE*, Universidade Federal do Rio de Janerio, Brazil.

18. A.C.M de Queiroz, "Mutual Inductance and Inductance Calculations by Maxwell's Method", *EE/COPPE* , Universidade Federal do Rio de Janerio, Brazil.

19. T. W. Barrett, "Tesla's Nonlinear Oscillator-shuttle-circuit (OSC) Theory", *Annales de la Fondation Louis de Broglie,* Vol. 16, No. 1, pg. 23, 1991.

20. A. Marincic, "Coupled Circuits Time and Frequency Analysis", *IEEE TELSIKS Symposium*, Serbia, 2007.

21. E.W. Herold, "Negative Resistance and Devices for Obtaining It", *Proceedings of the Institute of Radio Engineers*, Vol. 23, No. 10 pp. 1201, 1935.

22. A. M. Scalpi, *Crystal Oscillator Design and Negative Resistance*, Cypress Semiconductor, www.analogzone.com publications, 2005.

23. R.V Jones, *The Van der Pol Negative Resistance Oscillator*, http://people.seas.harvard.edu/~jones/ap216/lectures/ls_2/ls2_u6/vanderpol/ vanderpol.html, Mar 16 2000.

24. K.L. Corum and J.F. Corum, "RF Coils, Helical Resonators and Voltage Magnification by Coherent Spatial Modes", *IEEE TELSIKS,* 2001.

25. K.L. Corum, P.V. Pesavento and J.F. Corum, "Multiple Resonances in RF Coils and the Failure of Lumped Inductance Models", Oct. 2006, Sixth International Symposium Nikola Tesla, Belgrade Serbia.

26. G. Gorelik, "Resonance Phenomena in Linear Systems With Periodic Parameters", *Technical Physics of the USSR*, Leningrad; Vol. 2, No. 2-3, pp. 135-180, 1935.

27. R.R.A. Syms, L. Solymar, I.R. Young, "Three-frequency parametric amplification in magneto-inductive ring resonators", *Metamaterials*, Elsevier Science Direct, 2008.

28. A. Karalis, J.D. Joannopoulos, and Marin Soljačić, "Efficient wireless non-radiative mid-range energy transfer", http://arxiv.org/ftp/physics/papers/0611/0611063.htm, MIT, 2006.

29. S. Sensiper, *Electromagnetic Wave Propogation on Helical Conductors*, Technical Report No: 194, Research Laboratory of Electronics, MIT, 1951.

30. L.A. Harris, H.R. Johnson, A.Karp, L.D. Smullin, *Some Measurements of Phase Velocity Along a Helix With Dielectric Supports*, Technical Report No: 93, Research Laboratory of Electronics, MIT, 1949.

31. A. Tonning, *Propogation of an Electromagnetic Wave Along a Helix Surrounded by a Resistance Sheath*, Technical Report No: 232 Research Laboratory of Electronics, MIT, 1952.

32. S.H. Kogan, "Distribution of Waves Along an Infinite Helix", *Technical Physics Reports of the Academy of Sciences of the USSR*, Volume 66, No. 5, 1949.

33. J.R. Pierce, "Coupling of Modes in Helixes", *IEEE, Proceedings of the IRE*, Volume: 42, Issue: 9, pp. 1389, 1954.

34. S. Sensiper, "Electromagnetic Wave Propagation on Helical Structures" (A Review and Survey of Recent Progress), *IEEE, Proceedings of the IRE*, pp. 149, 1955.

35. W. Sichak, "Coaxial Line with Helical Inner Conductor", IEEE, *Proceedings of the IRE*, pp.1315, 1954.

36. D.C Wynn, C.T. Carson, "Numerical Computation of the Phase Velocity of Current on an Infinite Helix", *IEEE Electronics Letters*, Vol. 8 No 16 pp 424, 1972.

37. E. B. Perri, "Normal Mode Helical Monopole Antennas, Antennas and Propagation" *IEEE Society International Symposium*, 2008. AP-S 2008. Volume, Issue, 5-11 July, 2008.

39. L. Nichols, G. H. MacMaster, Slot Wave Coupling Circuit, US Patent No 4,349,791 Sep. 14, 1982.

40. F. Guerin, "Energy Dissipation and Absorption in Reciprocal Bi-Isotropic Media Described by Different Formalisms", *PIER 9*, 31-44, 1994.

41. J. Garnier, "Propogation and Amplification of Incoherent Pulses in Dispersive and Nonlinear Media", *Optical Society of America*, Vol. 15, No.11, pg. 2773, 1998.

42. M. D. Mermelstein, "A Magnetoelastic Metallic Glass Low-Frequency Magnetometer", *IEEE Transactions on Magnetics*, Vol. 28, No. 1, pg. 36, 1992.

43. A. J. Vijtanen and I. V. Lindell, "Chiral Slab Polarization Transformer for Aperture Antennas", *IEEE Transactions on Antennas and Propagation*, Vol. 46, No. 9, 1998.

44. A. Vijtanen, "Chiral Mode Transformer for Hard Surface Waveguides", *IEEE 29th Microwave Conference,* Munich, 1999.

45. ICNIRP Guidelines, "Guidelines for Limiting Exposure to Time-varying Electric, Magnetic, and Electromagnetic Fields (Up to 300GHz)", *International Commission on Non-Ionizing Radiation Protection*, Health Physics Society, pg 494, 1998.

46. *Field Service Memo Electromagnetic Radiation and How it Affects Your Instruments* http://www.osha.gov/SLTC/radiofrequencyradiation/electromagnetic_fieldmemo/ electromagnetic.html